

SEISMOLOGY I

Laurea Magistralis in Physics of the Earth and of the Environment

Free modes of the Earth

Fabio ROMANELLI

Dept. Earth Sciences

Università degli studi di Trieste

romanel@dst.units.it

Surface Waves and Free Oscillations

Surface waves in an elastic half spaces: Rayleigh waves

- Potentials
- Free surface boundary conditions
- Solutions propagating along the surface, decaying with depth
- Lamb's problem

Surface waves in media with depth-dependent properties: Love waves

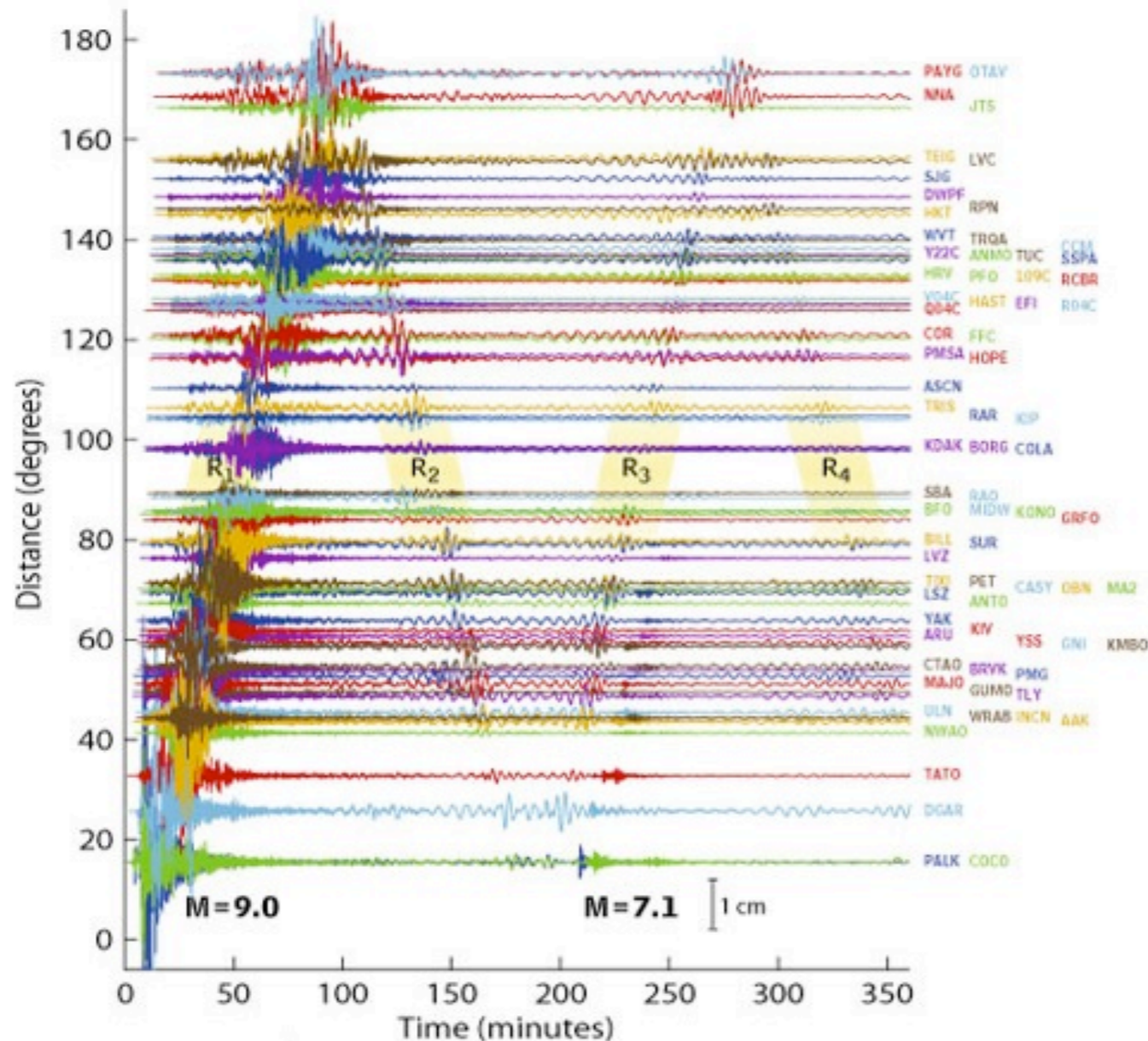
- Constructive interference in a low-velocity layer
- Dispersion curves
- Phase and Group velocity

Free Oscillations

- Spherical Harmonics
- Modes of the Earth
- Rotational Splitting

Traveling surface waves

Sumatra - Andaman Islands Earthquake ($M_w=9.0$)
Global Displacement Wavefield from the Global Seismographic Network



Vertical displacements of the Earth's surface recorded by seismometers.

The traces are arranged by distance from the epicenter in degrees. The earliest, lower amplitude, signal is that of the compressional (P) wave, which takes about 22 minutes to reach the other side of the planet (the antipode).

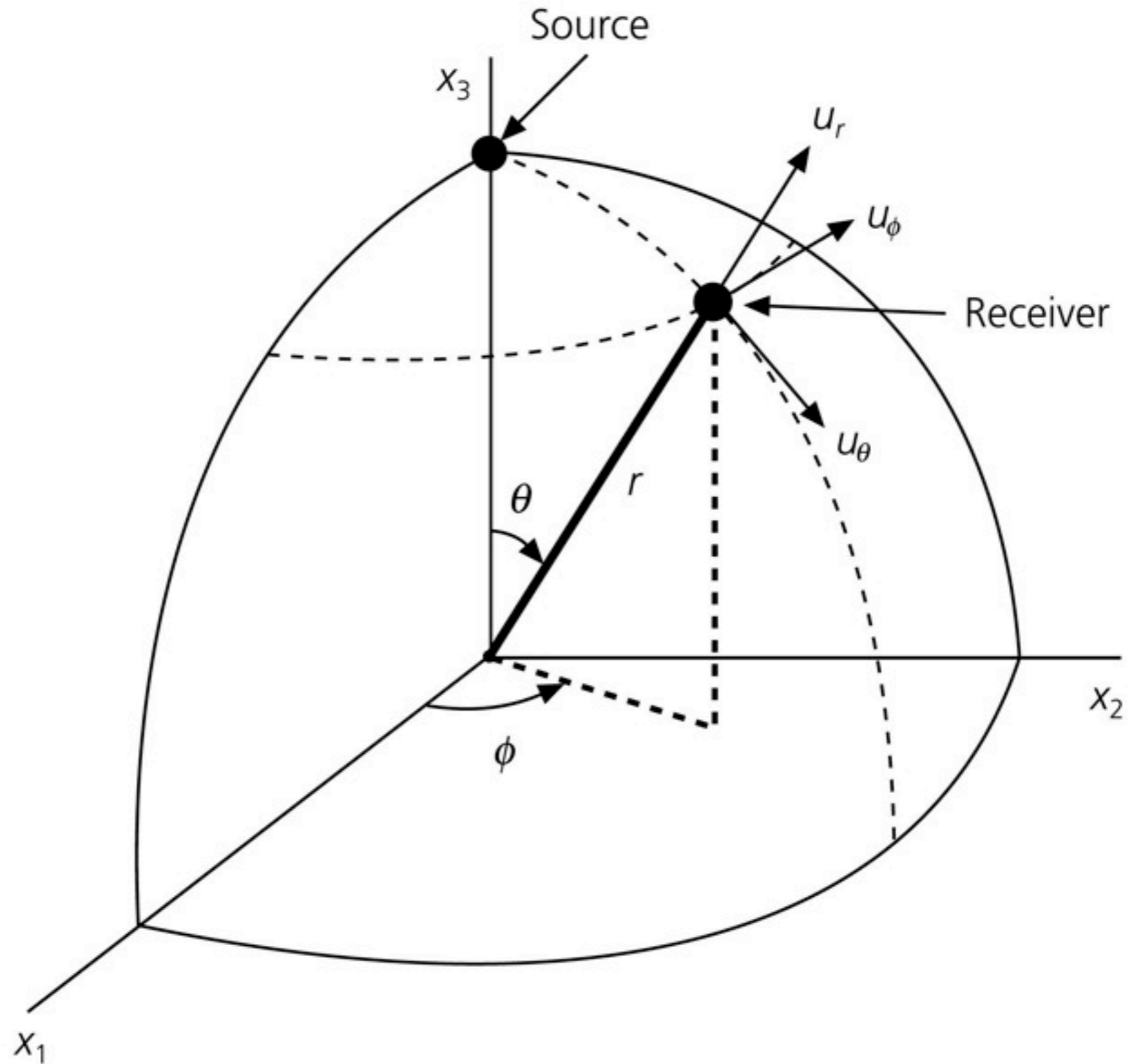
The largest amplitude signals are seismic surface waves that reach the antipode after about 100 minutes. The surface waves can be clearly seen to reinforce near the antipode (with the closest seismic stations in Ecuador), and to subsequently circle the planet to return to the epicentral region after about 200 minutes.

A major aftershock (magnitude 7.1) can be seen at the closest stations starting just after the 200 minute mark (note the relative size of this aftershock, which would be considered a major earthquake under ordinary circumstances, compared to the mainshock).



Spherical geometry

Figure 2.9-1: Spherical coordinate geometry for normal modes.



Wave equation & Laplacian

- Wave equation

$$v^2 \nabla^2 \mathbf{u} = v^2 \Delta \mathbf{u} = \mathbf{u}_{tt}$$

- Laplacian in Spherical system

$$\Delta f = \frac{1}{r^2} \frac{\partial}{\partial r} \left(r^2 \frac{\partial f}{\partial r} \right) + \frac{1}{r^2 \sin \theta} \frac{\partial}{\partial \theta} \left(\sin \theta \frac{\partial f}{\partial \theta} \right) + \frac{1}{r^2 \sin^2 \theta} \frac{\partial^2 f}{\partial \varphi^2}$$

Separation of variables

$$u(r, \theta, \phi, t) = R(r)\Theta(\theta)\Phi(\phi)T(t)$$

$$\Phi''(\phi) + m^2\Phi(\phi) = 0$$

$$\Phi(\phi) = C \cos(m\phi) + D \sin(m\phi)$$

m is a positive integer

$$T''(t) + c^2 k^2 T(t) = 0$$

$$T(t) = A \cos(\omega t) + B \sin(\omega t)$$

$\omega = ck$

$$\frac{1}{\sin\theta} \frac{d}{d\theta} \left(\sin\theta \frac{d\Theta}{d\theta} \right) + \left[l(l+1) - \frac{m^2}{\sin^2\theta} \right] \Theta = 0$$

$$\frac{1}{r^2} \frac{\partial}{\partial r} \left(r^2 \frac{dR}{dr} \right) + \left[k^2 - \frac{l(l+1)}{r^2} \right] R = 0$$

Legendre polynomials

Spherical harmonics: defined by an orthogonal set of functions called Legendre Polynomials

θ = angular distance from the pole (colatitude)

ϕ = azimuth around the pole (longitude)

Legendre polynomials:
$$P_l(x) = \frac{1}{2^l l!} \frac{d^l}{dx^l} (x^2 - 1)^l$$

l = degree, or angular order

The first several polynomials are

$$P_0(x) = 1$$

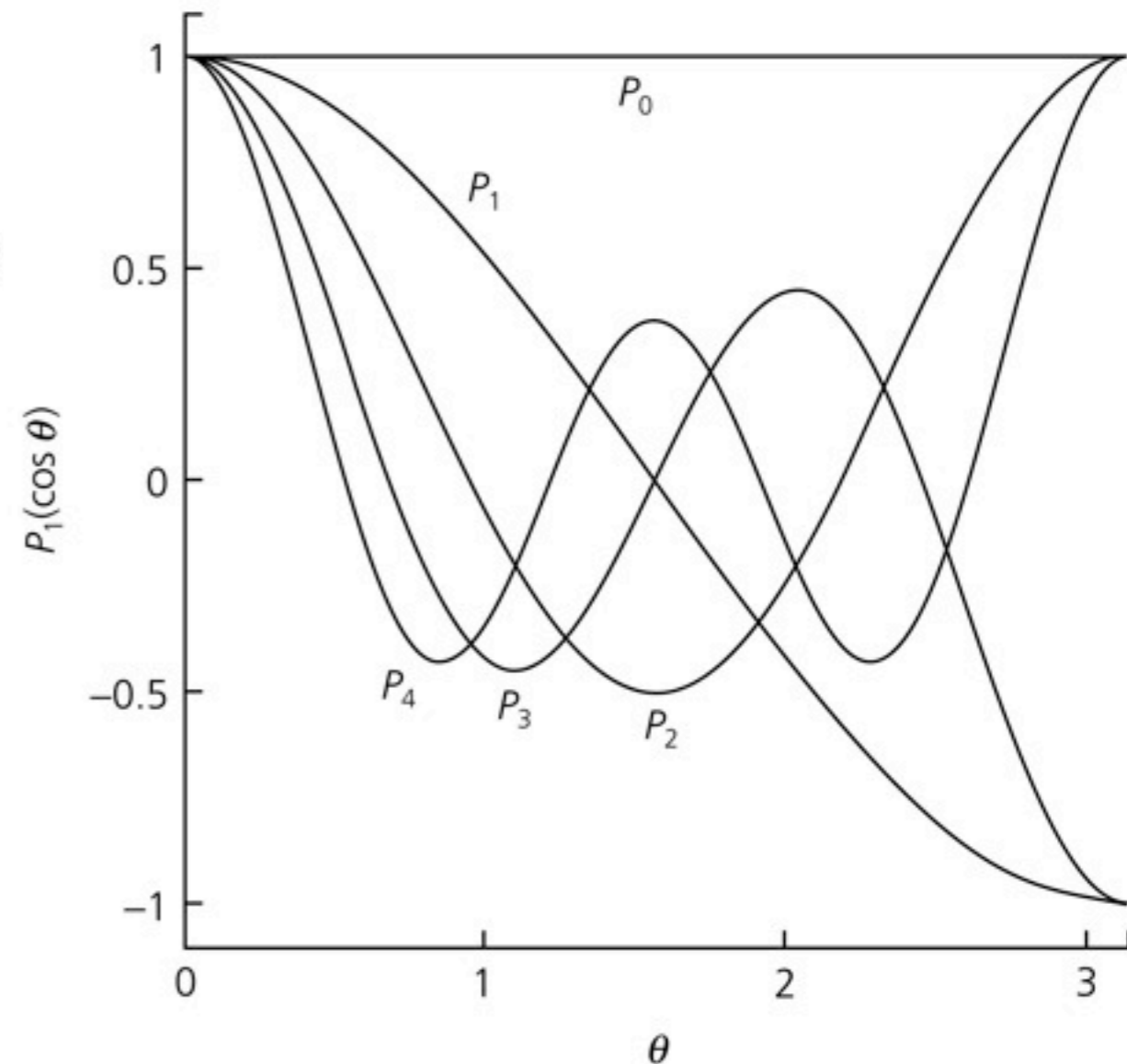
$$P_1(x) = x$$

$$P_2(x) = (1/2)(3x^2 - 1)$$

$$P_3(x) = (1/2)(5x^3 - 3x)$$

On a sphere, $x = \cos \theta$ so x ranges from $-1 \leq x \leq 1$

Figure 2.9-3: Examples of Legendre polynomials.



Spherical harmonics

The azimuthal variations are included by forming the *Associated Legendre functions*,

$$P_l^m(x) = \left[\frac{(1-x^2)^{m/2}}{2^l l!} \right] \left[\frac{d^{l+m}}{dx^{l+m}} (x^2-1)^l \right]$$

(the *azimuthal order*, m , varies over $-l \leq m \leq l$)

Fully normalized spherical harmonics:

$$Y_l^m(\theta, \phi) = (-1)^m \left[\left(\frac{2l+1}{4\pi} \right) \frac{(l-m)!}{(l+m)!} \right]^{1/2} P_l^m(\cos\theta) e^{im\phi}$$

In mathematics, the **spherical harmonics** are the angular portion of an orthogonal set of solutions to Laplace's equation represented in a system of spherical coordinates.

Spherical harmonics are orthogonal:

$$\int_0^{2\pi} \int_0^{\pi} \sin \theta Y_l^{m'*}(\theta, \phi) Y_l^m(\theta, \phi) d\theta d\phi = \delta_{l'l} \delta_{m'm}$$

The spherical harmonics are easily visualized by counting the number of zero crossings they possess in both the latitudinal and longitudinal directions. For the latitudinal direction, the associated Legendre functions possess $l - |m|$ zeros, whereas for the longitudinal direction, the trigonometric sin and cos functions possess $2|m|$ zeros.

When the spherical harmonic order m is zero, the spherical harmonic functions do not depend upon longitude, and are referred to as **zonal**. When $l = |m|$, there are no zero crossings in latitude, and the functions are referred to as **sectoral**. For the other cases, the functions checker the sphere, and they are referred to as **tesseral**.

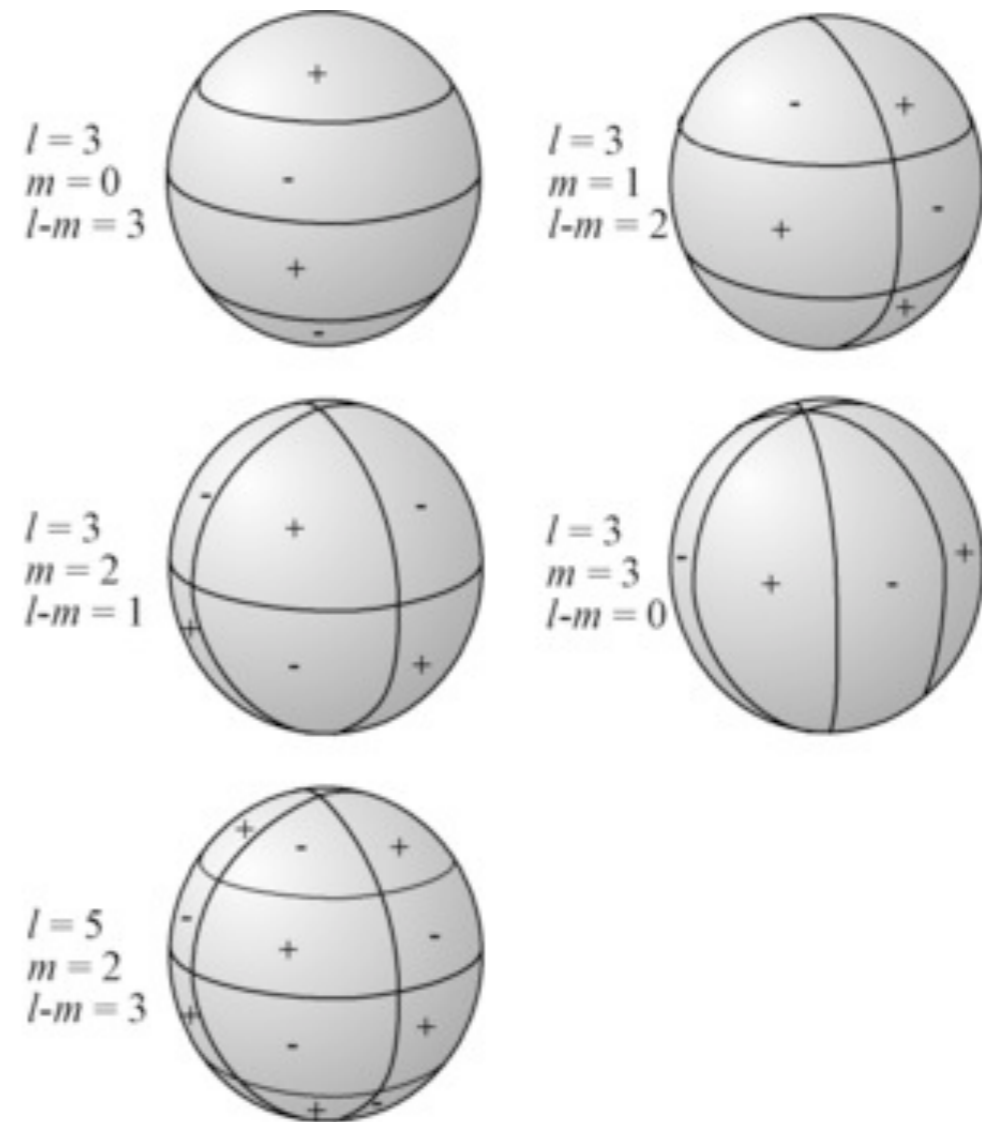
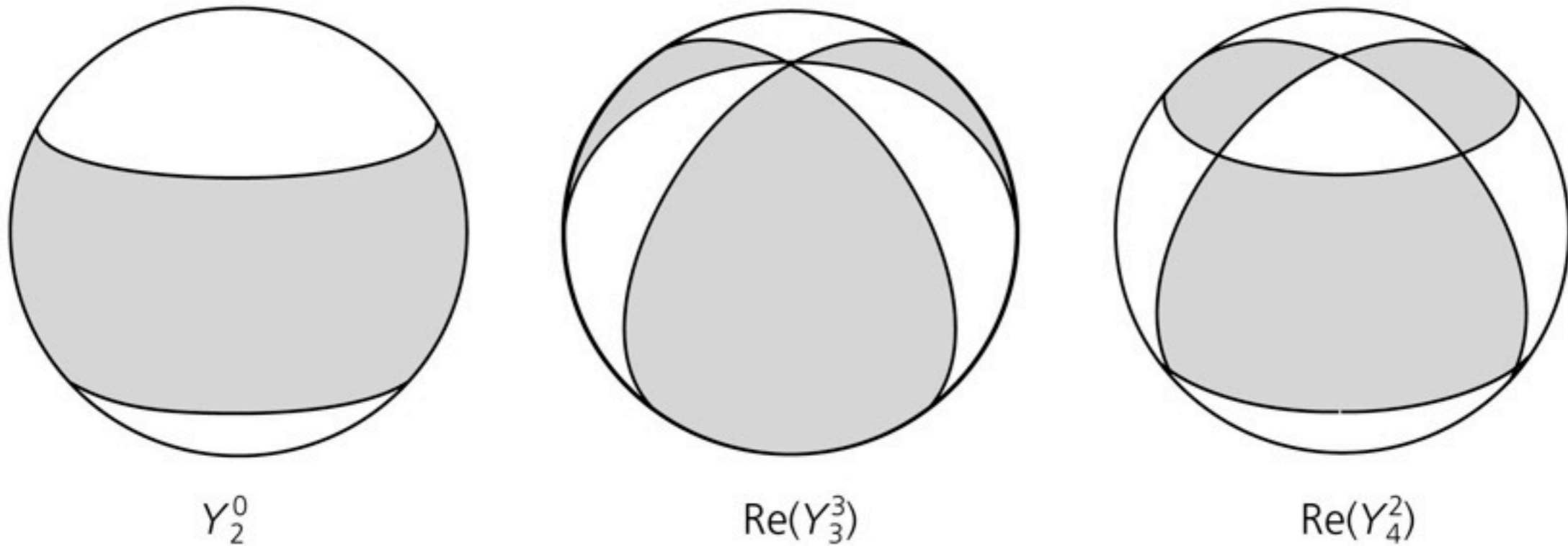


Figure 2.9-4: Examples of spherical harmonics.



$$Y_l^m(\theta, \phi) = (-1)^m \left[\left(\frac{2l+1}{4\pi} \right) \frac{(l-m)!}{(l+m)!} \right]^{1/2} P_l^m(\cos\theta) e^{im\phi}$$

The angular order, l , gives the number of nodal lines on the surface.

If the azimuthal order m is zero, the nodal lines are small circles about the pole. These are called *zonal* harmonics, and do not depend on ϕ

If $m = l$, then all of the surface nodal lines are great circles through the pole. These are called *sectoral* harmonics.

When $0 < |m| < l$, there are combined angular and azimuthal (colatitudinal and longitudinal) nodal patterns called *tesseral* harmonics.

Torsional & Spheroidal modes

Torsional modes ${}_nT_l^m$:

- * No radial component: tangential only, normal to the radius: motion confined to the surface of n concentric spheres inside the Earth (**SH, Love waves**).
- * Changes in the shape, not of volume
- * Do not exist in a fluid: so only in the mantle (and the inner core?)

n - radial : nodal planes with depth
 l - polar : # nodal planes in latitude
! Max nodal planes = $l - 1$
 m - azimuthal : # nodal planes in longitude

Spheroidal modes ${}_nS_l^m$:

- * Horizontal components (tangential) et vertical (radial) (**P-SV, Rayleigh waves**)
- * No simple relationship between n and nodal spheres
- * ${}_0S_2$ is the longest "fundamental"
- * Affect the whole Earth (even into the fluid outer core !)

n : no direct relationship with nodes with depth
 l : # nodal planes in latitude
! Max nodal planes = l
 m : # nodal planes in longitude

Torsional modes

Torsional (toroidal) modes:
(analogous to SH waves)



Surface eigenfunctions given by vector spherical harmonics:

$$\mathbf{T}_l^m(r, \theta, \phi) = \left(0, \frac{1}{\sin \theta} \frac{\partial Y_l^m(\theta, \phi)}{\partial \phi}, -\frac{\partial Y_l^m(\theta, \phi)}{\partial \theta} \right)$$

The displacements are given by:

$$\mathbf{u}^T(r, \theta, \phi) = \sum_n \sum_l \sum_{m=-l}^l {}_n A_l^m {}_n W_l(r) \mathbf{T}_l^m(\theta, \phi) e^{i \omega_l^m t}$$

${}_n W_l(r)$ - The radial eigenfunction (varies with depth)



For ${}_nT_l^m$:

n = radial order, l = angular order, m = azimuthal order.

The $2l + 1$ modes of different azimuthal orders $-l \leq m \leq l$ are called *singlets*, and the group of singlets is called a *multiplet*.

If earth were perfectly spherically symmetric and non-rotating, all singlets in a multiplet would have the same eigenfrequency (called *degeneracy*).

For example, the period of ${}_nT_l^0$ would be the same for ${}_nT_l^{\pm 1}$, ${}_nT_l^{\pm 2}$, ${}_nT_l^{\pm 3}$, etc. In the real earth, singlet frequencies vary (called *splitting*).

The splitting is usually small enough to ignore, so we drop the m superscript and refer to the entire ${}_nT_l^m$ multiplet as ${}_nT_l$, with eigenfrequency ${}_n\omega_l$.



Example:

$$Y_l^m(\theta, \phi) = (-1)^m \left[\left(\frac{2l+1}{4\pi} \right) \frac{(l-m)!}{(l+m)!} \right]^{1/2} P_l^m(\cos\theta) e^{im\phi}$$

$$\mathbf{T}_l^m = \left(0, \frac{1}{\sin\theta} \frac{\partial Y_l^m(\theta, \phi)}{\partial \phi}, -\frac{\partial Y_l^m(\theta, \phi)}{\partial \theta} \right)$$

$$e^{im\phi} \frac{\partial}{\partial \theta} P_2^0(\cos\theta) = 3 \sin\theta \cos\theta$$

Figure 2.9-5: Displacement associated with torsional mode ${}_0T_2^0$.

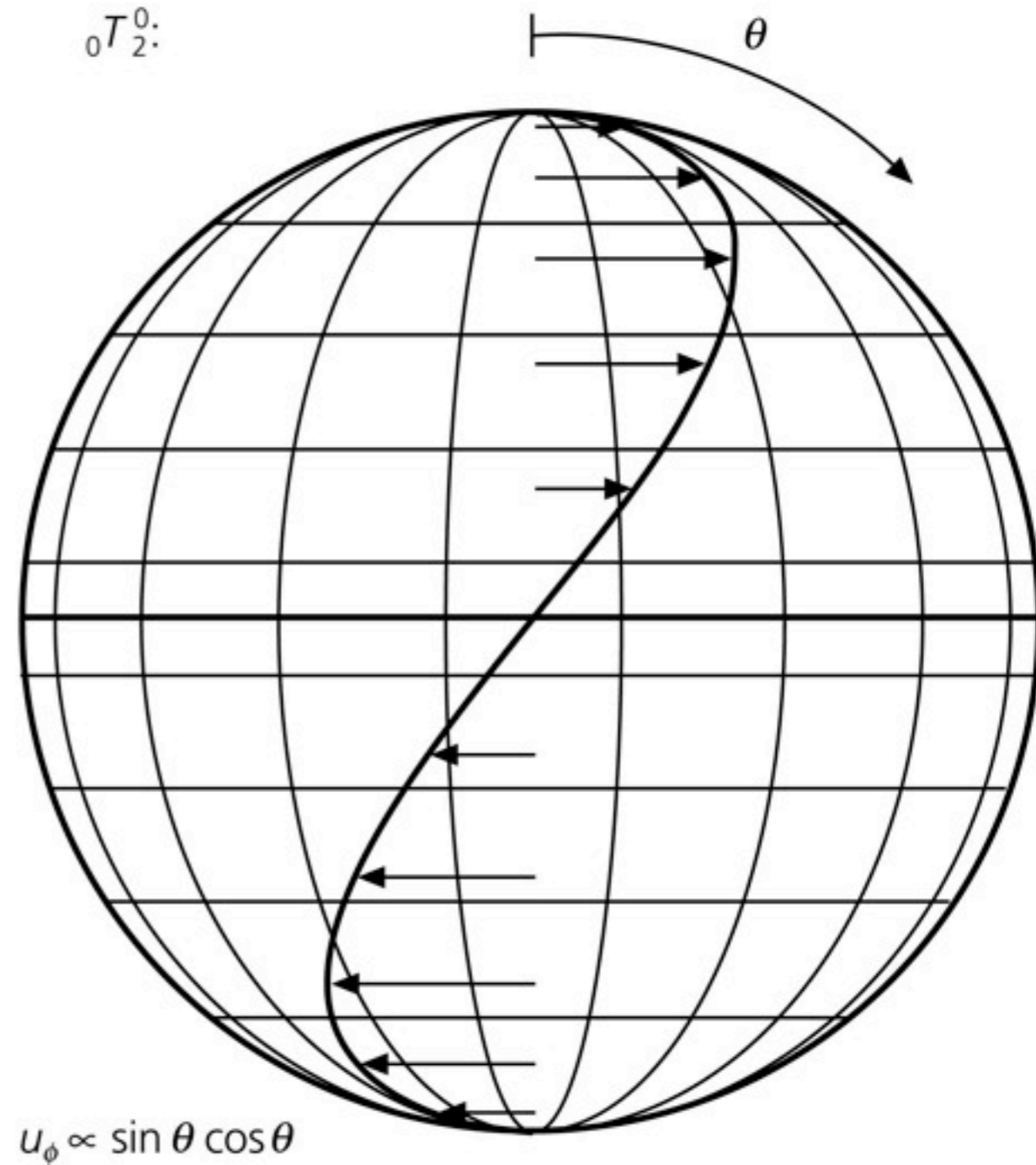


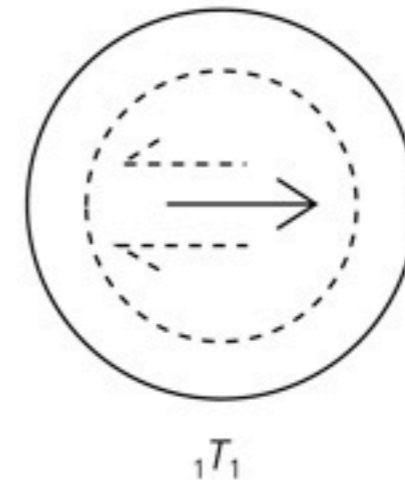
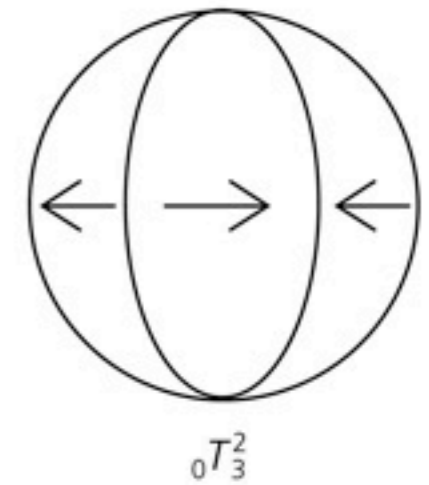
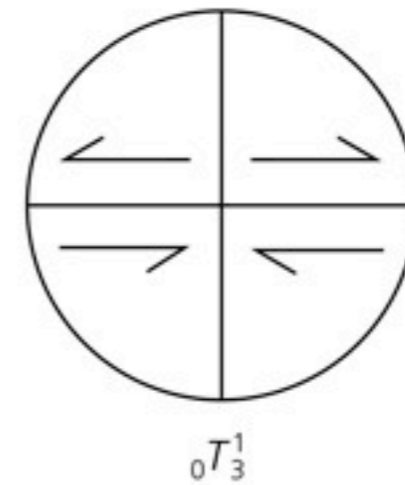
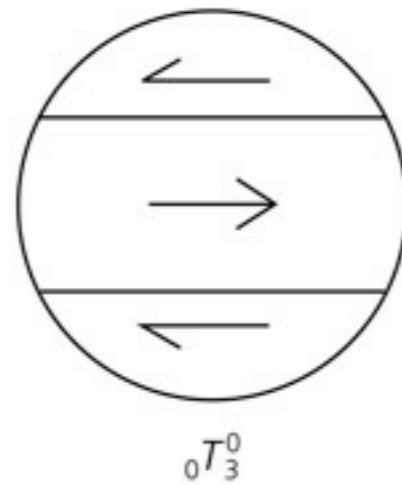
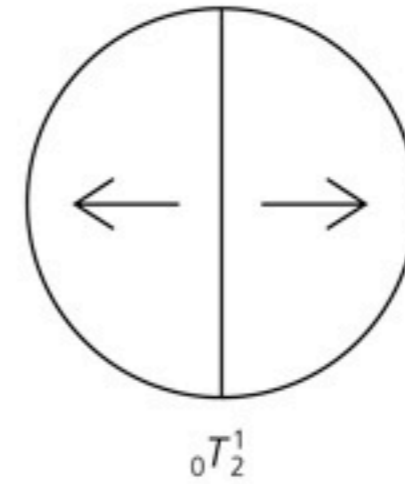
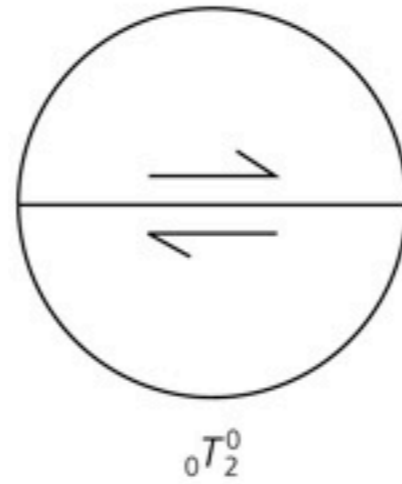


Figure 2.9-6: Examples of the displacements for several torsional modes.

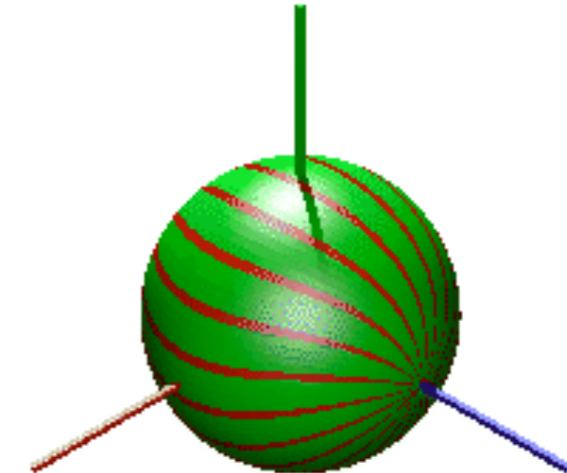
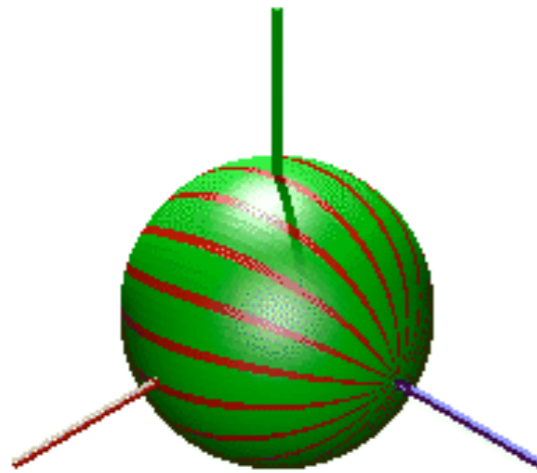
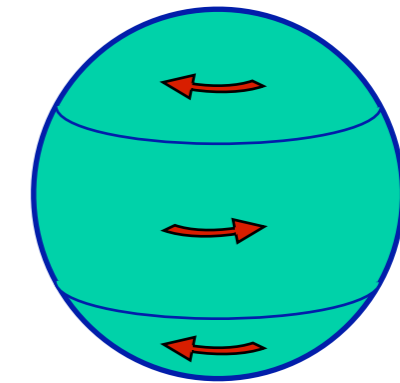
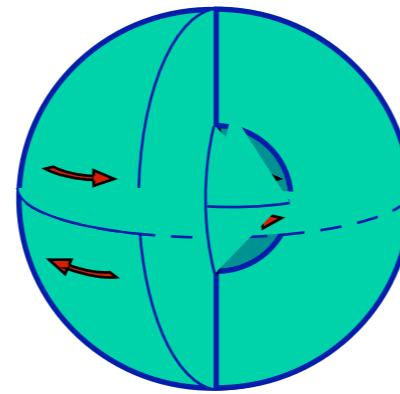
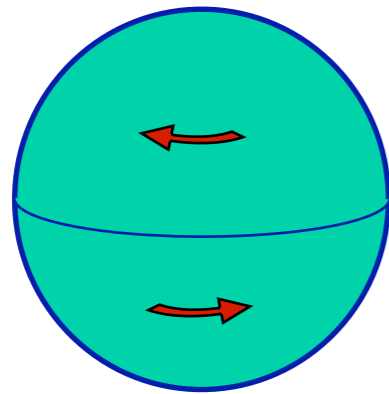
Torsional modes with $n = 0$ (${}_0T_l^m$) are called *fundamental modes*. (motions at depth in the same direction as at the surface).

Modes with $n > 0$ are called *overtones*. (motions reverse directions at different depths)

What happened to ${}_0T_1$ and ${}_0T_0$?



Toroidal normal modes: examples



${}_0T_2$: «twisting» mode

${}_1T_2$

${}_0T_3$

(44.2 minutes, observed in
1989 with an extensometer)

(12.6 minutes)

(28.4 minutes)

Animations from Lucien Saviot

<http://www.u-bourgogne.fr/REACTIVITE/manapi/saviot/deform/>

Spheroidal modes

Spheroidal (poloidal) modes (involving P - SV motions):

The surface eigenfunctions are given by two other *vector spherical harmonics* with (r, θ, ϕ) components

$$\mathbf{R}_l^m = (Y_l^m, 0, 0)$$

$$\mathbf{S}_l^m = \left(0, \frac{\partial Y_l^m(\theta, \phi)}{\partial \theta}, \frac{1}{\sin \theta} \frac{\partial Y_l^m(\theta, \phi)}{\partial \phi} \right)$$

Each corresponds to a different radial eigenfunction, ${}_n U_l(r)$ and ${}_n V_l(r)$, so the displacement for spheroidal modes is

$$\mathbf{u}^S(r, \theta, \phi) = \sum_n \sum_l \sum_{m=-l}^l {}_n A_l^m \left[{}_n U_l(r) \mathbf{R}_l^m(\theta, \phi) + {}_n V_l(r) \mathbf{S}_l^m(\theta, \phi) \right] e^{i\omega_l^m t}$$

The radial eigenfunction ${}_n U_l(r)$ corresponds to radial motion and ${}_n V_l(r)$ corresponds to horizontal motion.

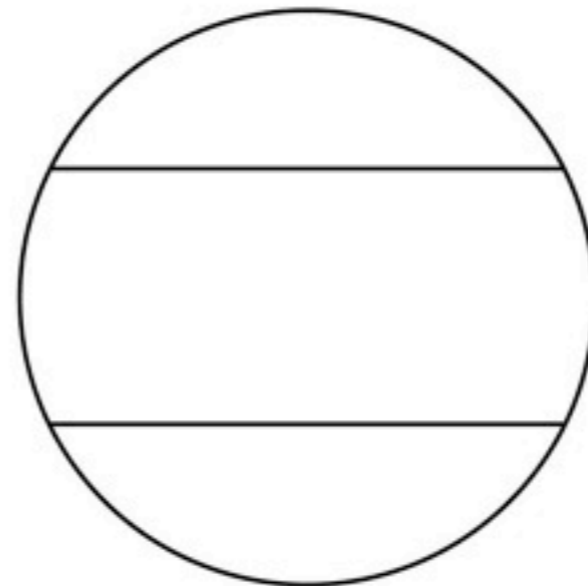


Figure 2.9-7: Examples of the displacements for several spheroidal modes.

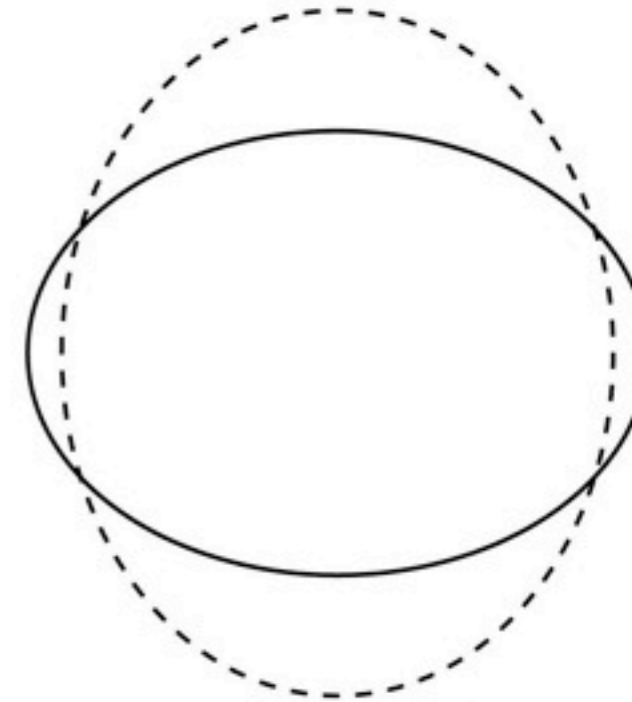
${}_0S_2$ (football mode) is the gravest (lowest frequency or longest period) of earth's modes, with a period of 3233 s, or 54 minutes.

There is no ${}_0S_1$ mode, which would correspond to a lateral translation of the planet.

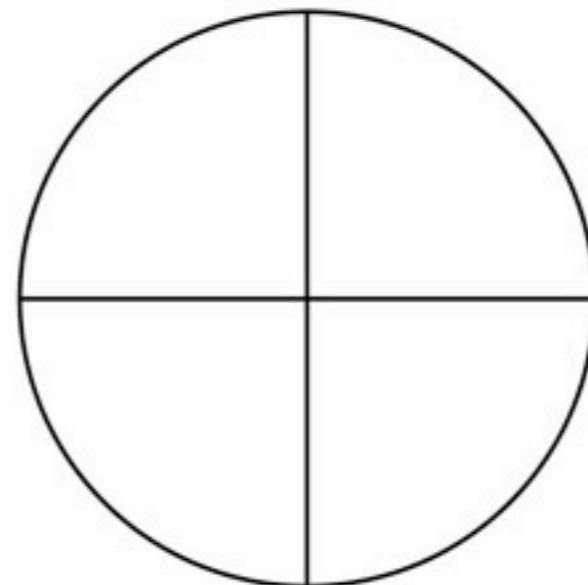
The ${}_1S_1$ Slichter mode due to lateral sloshing of the inner core through the liquid iron outer core, which has yet to be observed, should in theory have a period of about 5 1/2 hours.



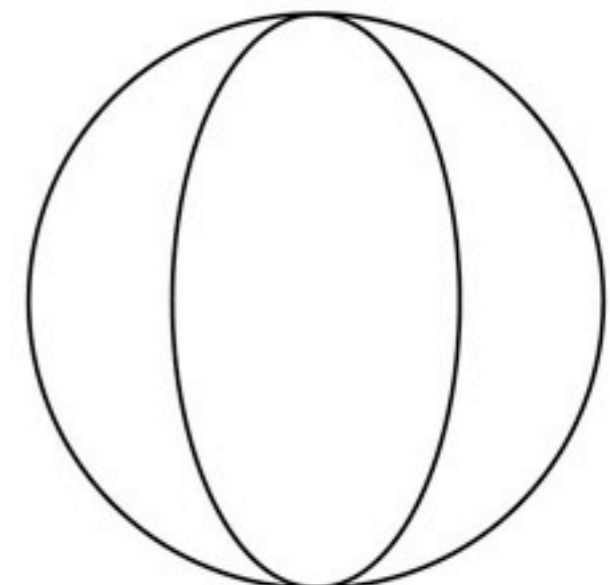
${}_0S_2^0$



${}_0S_2^0$ (motion)



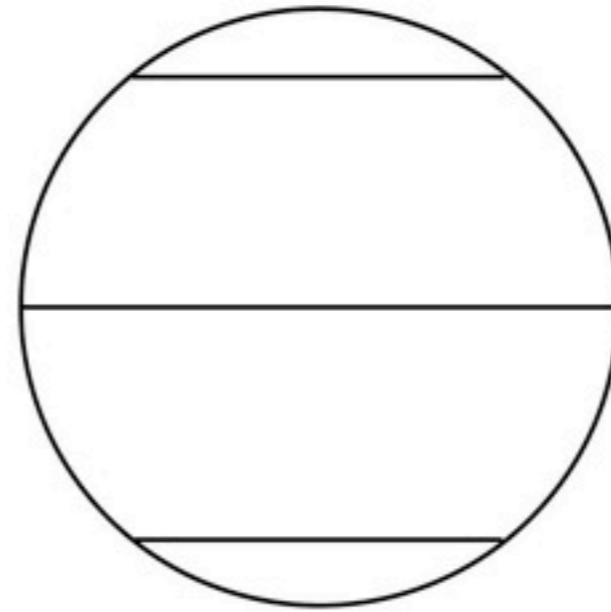
${}_0S_2^1$



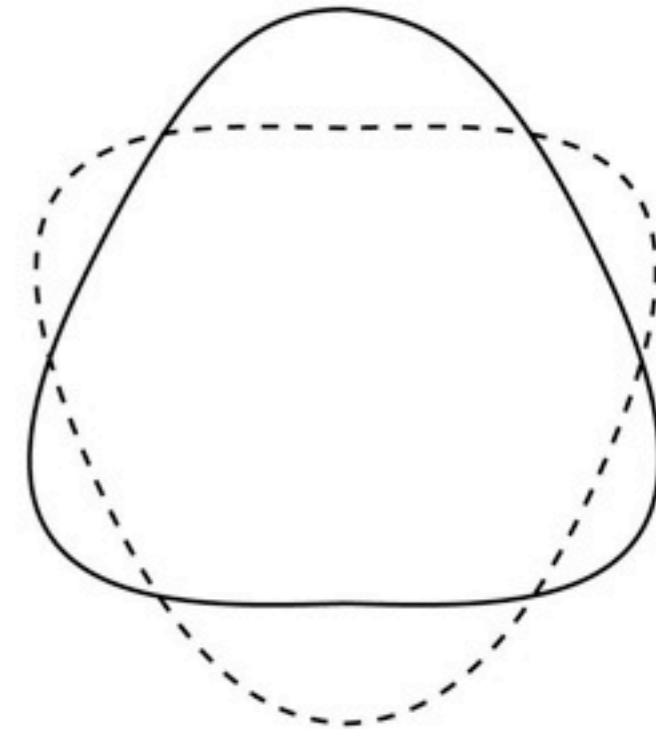
${}_0S_2^2$



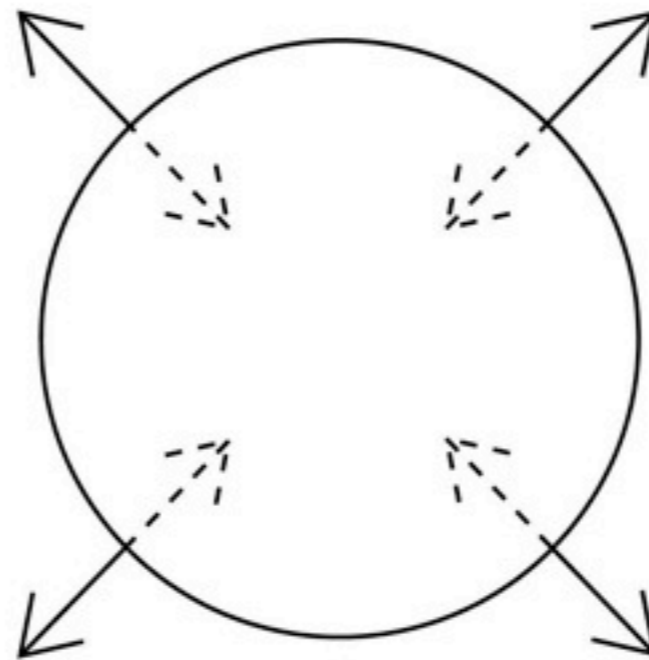
The "breathing" mode ${}_0S_0$ involves radial motions of the entire earth that alternate between expansion and contraction.



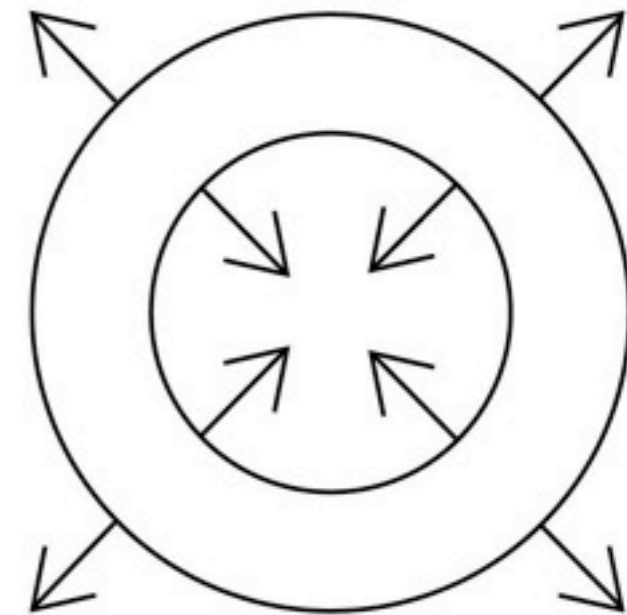
${}_0S_3$



${}_0S_3$ (motion)

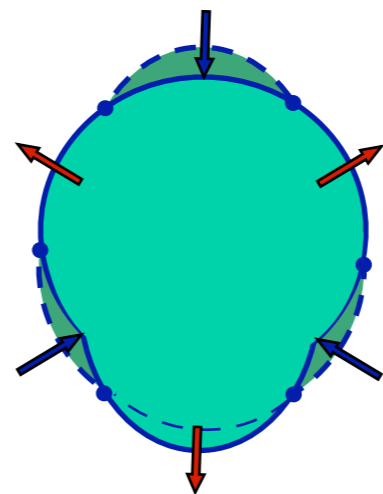
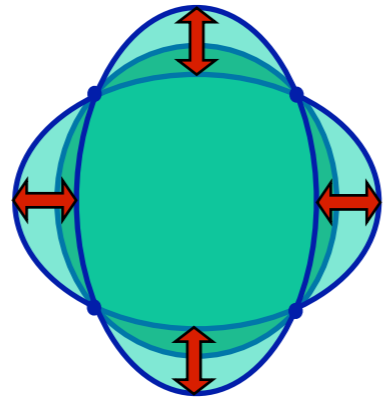
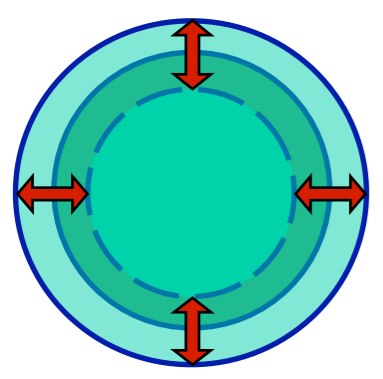


${}_0S_0$

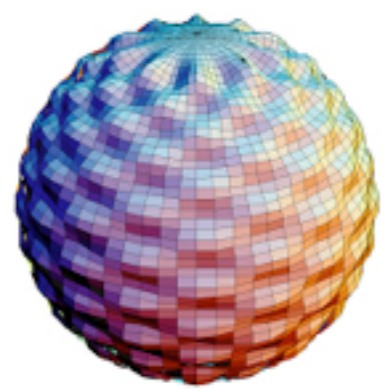


${}_1S_0$

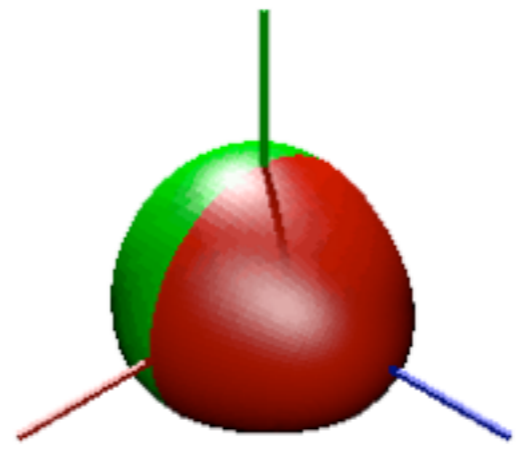
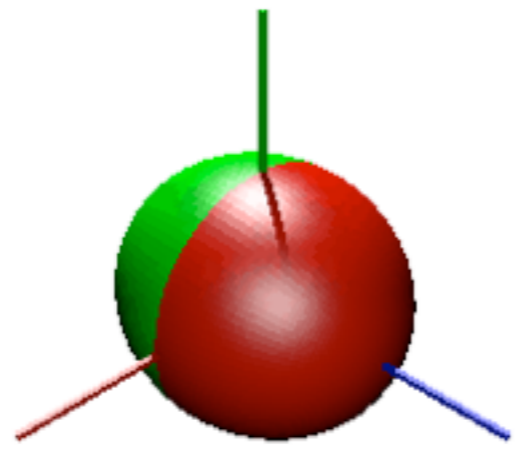
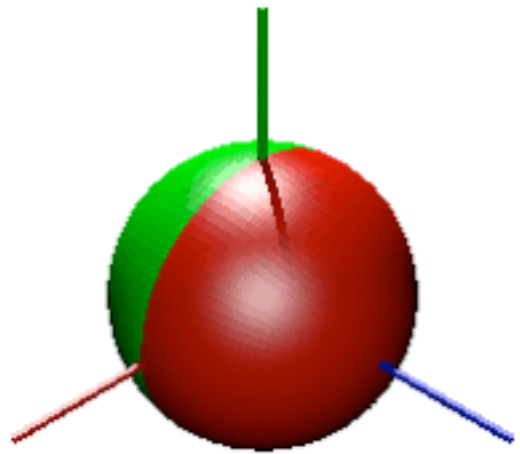
Spheroidal normal modes: examples



...



...



${}_0S_0$: « balloon » or
« breathing » :
radial only
(20.5 minutes)

${}_0S_2$: « football » mode
(Fundamental, 53.9
minutes)

${}_0S_3$:
(25.7 minutes)

...

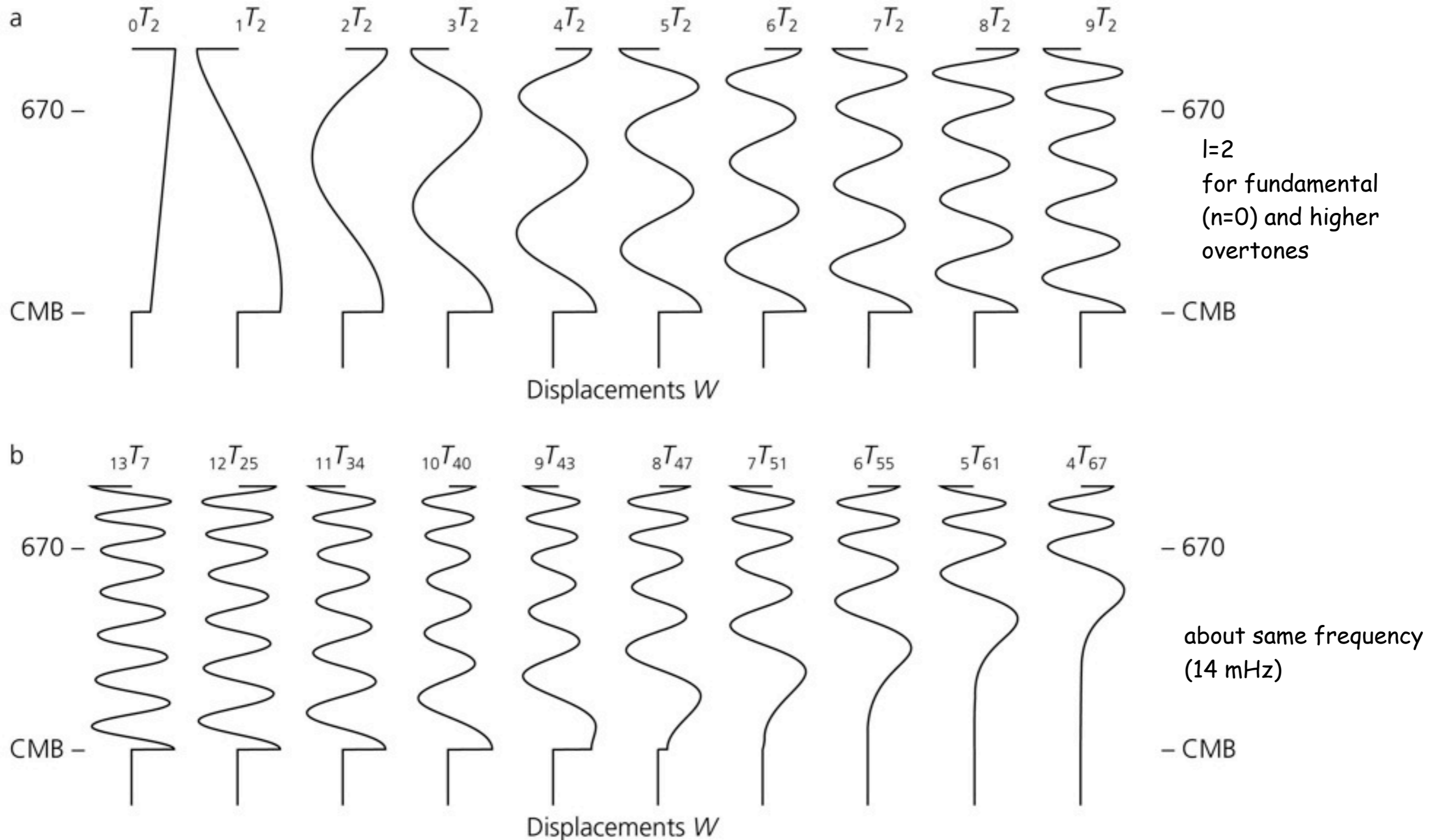
${}_0S_{29}$:
(4.5 minutes)

Animations from Lucien Saviot
<http://www.u-bourgogne.fr/REACTIVITE/manapi/saviot/deform/>

See also Animations from Hein Haak
<http://www.knmi.nl/kenniscentrum/eigentrillingen-sumatra.html>

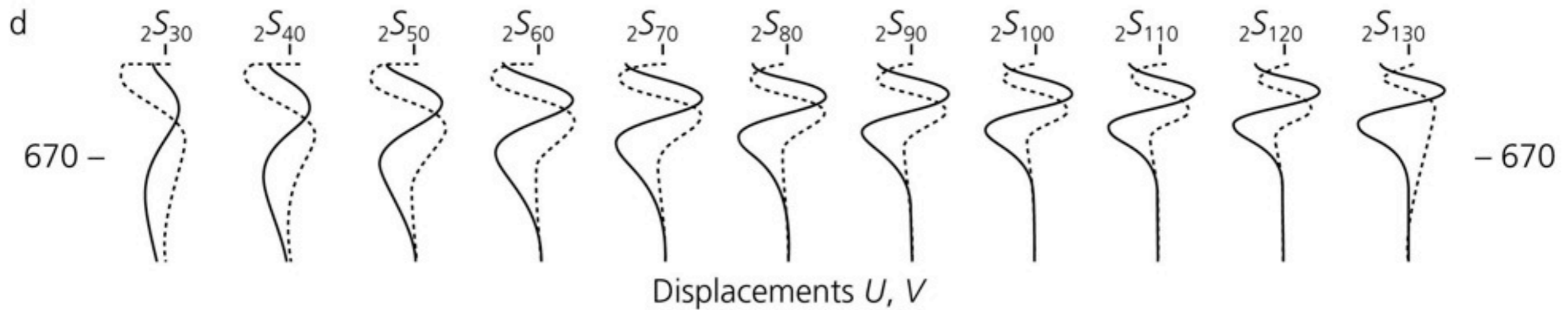
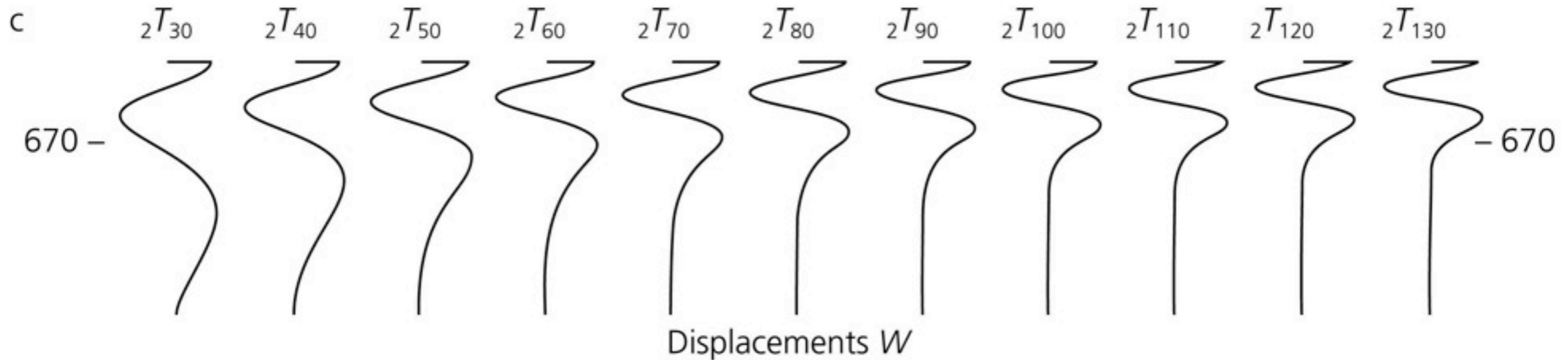
Torsional eigenfunctions

Figure 2.9-9: Radial eigenfunctions for various modes.



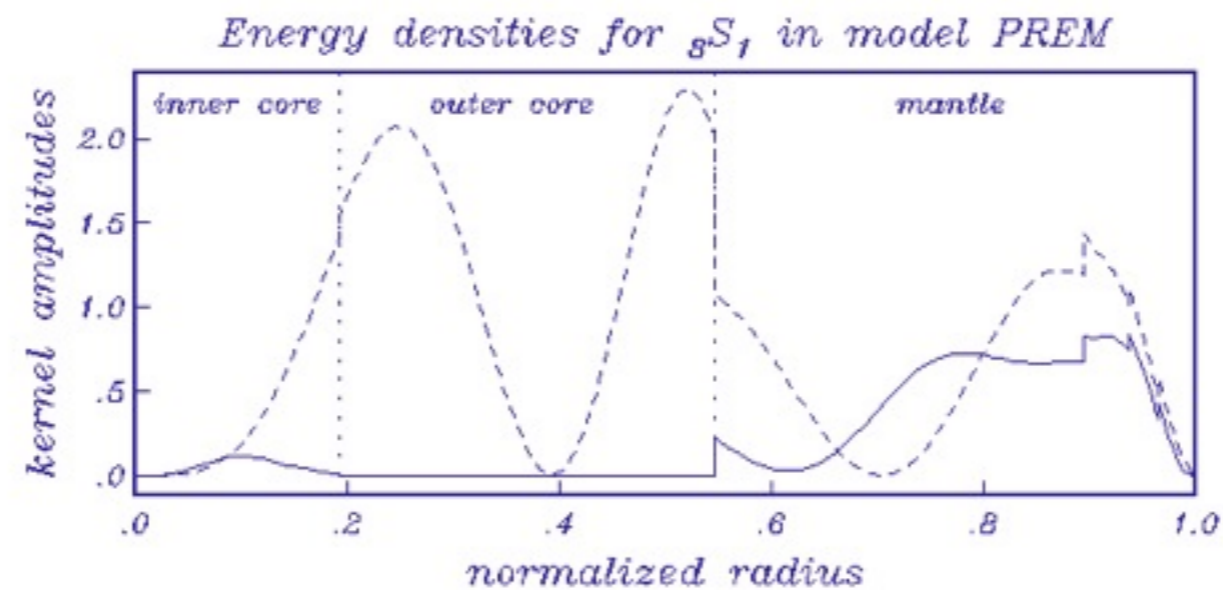
Spheroidal & Torsional eigenfunctions

second overtone branch



second overtone branch

One of the modes used in 1971 to infer the solidity of the inner core:
Part of the shear and compressional energy in the inner core

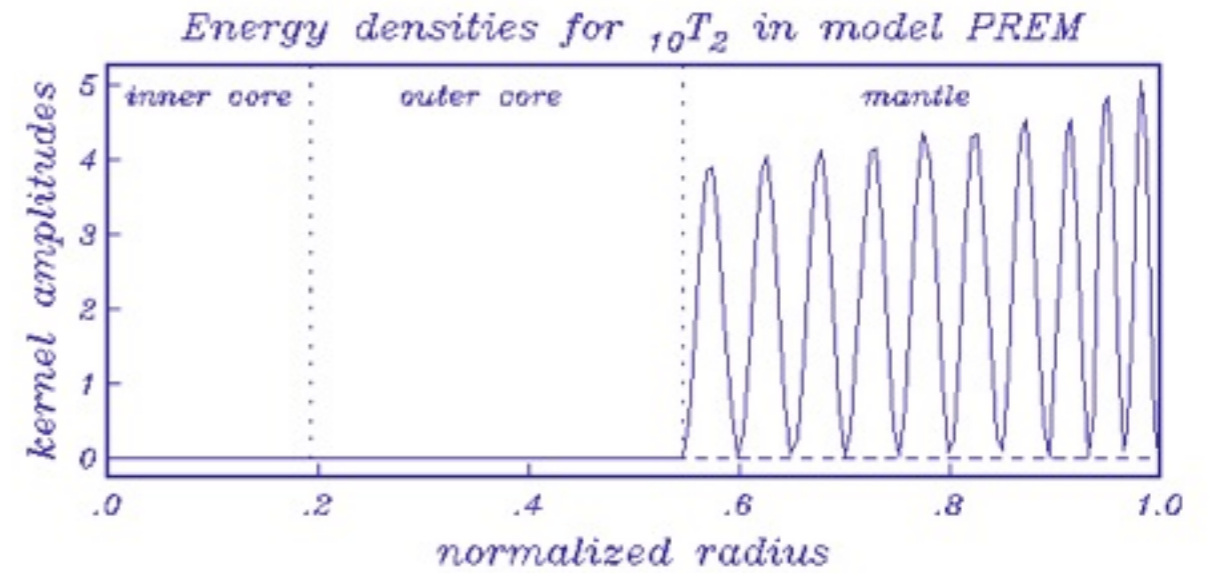
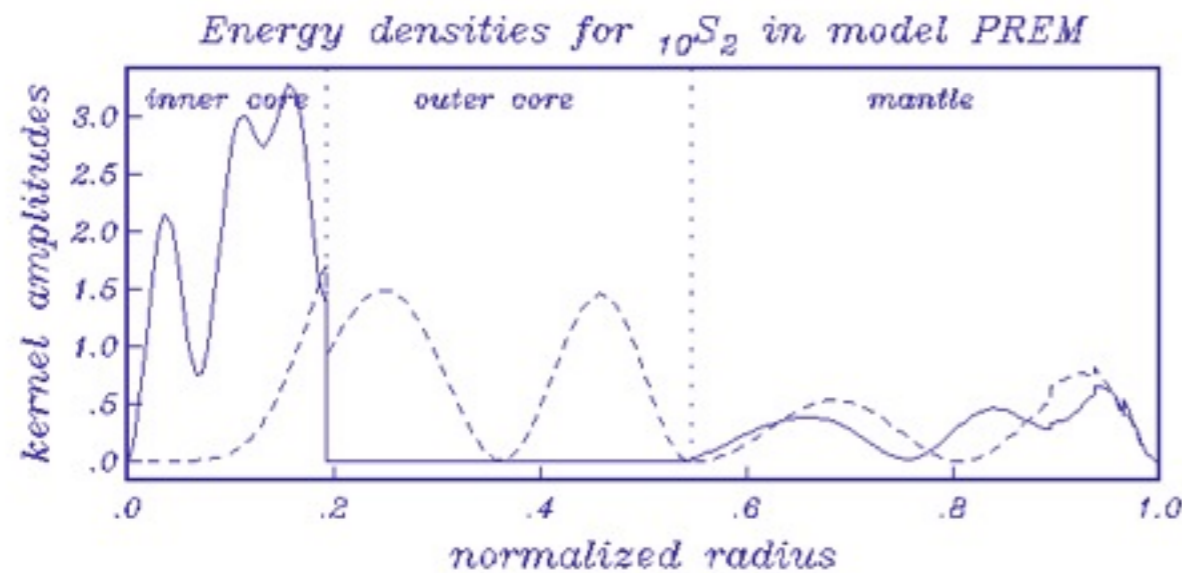
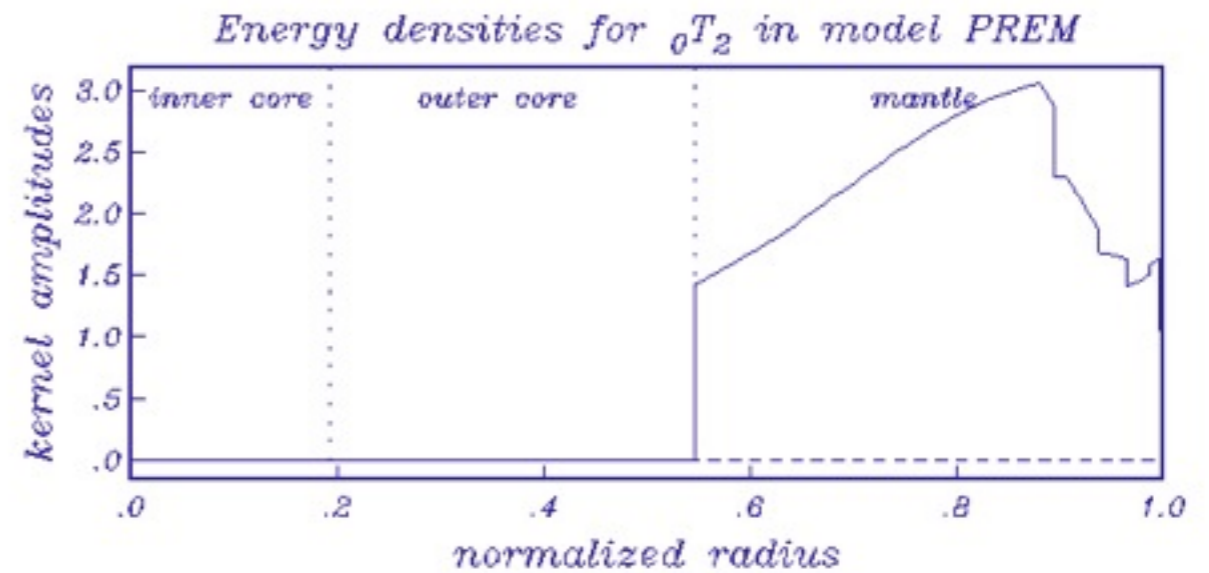
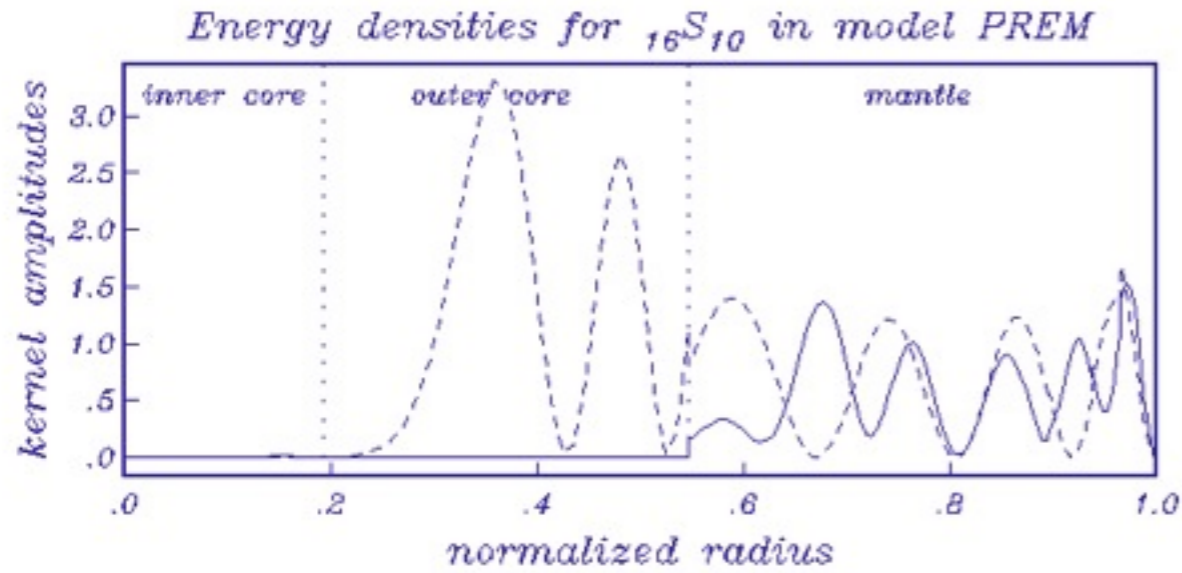


———— shear energy density
----- compressional energy density

Ruedi Widmer's home page:

<http://www-gpi.physik.uni-karlsruhe.de/pub/widmer/Modes/modes.html>

S can affect the whole Earth (esp. overtones) T in the mantle only !



———— shear energy density
 - - - - - compressional energy density

Eigenvalues

Some toroidal and spheroidal modes.

Mode	Period (s)	Description or associated phase
${}_0T_2$	2639.4	fundamental toroidal
${}_0T_3$	1707.6	fundamental toroidal
${}_1T_1$	808.4	radial overtone
${}_1T_2$	757.5	radial overtone
${}_9T_2$	104.4	radial overtone
${}_0T_{30}$	259.5	fundamental Love
${}_0T_{130}$	68.9	fundamental Love
${}_2T_{30}$	151.3	second-overtone Love
${}_4T_{67}$	71.3	SH
${}_{10}T_{40}$	71.4	SH_{diff}
${}_{13}T_7$	71.6	ScS_{SH}
${}_0S_0$	1228.1	fundamental radial
${}_1S_0$	613.0	radial overtone
${}_0S_2$	3233.5	football
${}_0S_3$	2134.4	pear-shaped
${}_0S_{30}$	262.1	fundamental Rayleigh
${}_0S_{130}$	75.8	fundamental Rayleigh
${}_1S_{30}$	160.9	second-overtone Rayleigh
${}_{10}S_6$	203.5	inner core $PKJKP$
${}_{11}S_5$	197.1	inner core $PKIKP$
${}_{14}S_3$	184.9	mantle ScS_{SV}
${}_1S_1$	19500	Slichter

Mid-1800's – music of the spheres – Earth's revolution is a C#, 33 octaves below middle C#

(breathing mode is an E, 20 octaves below middle E)

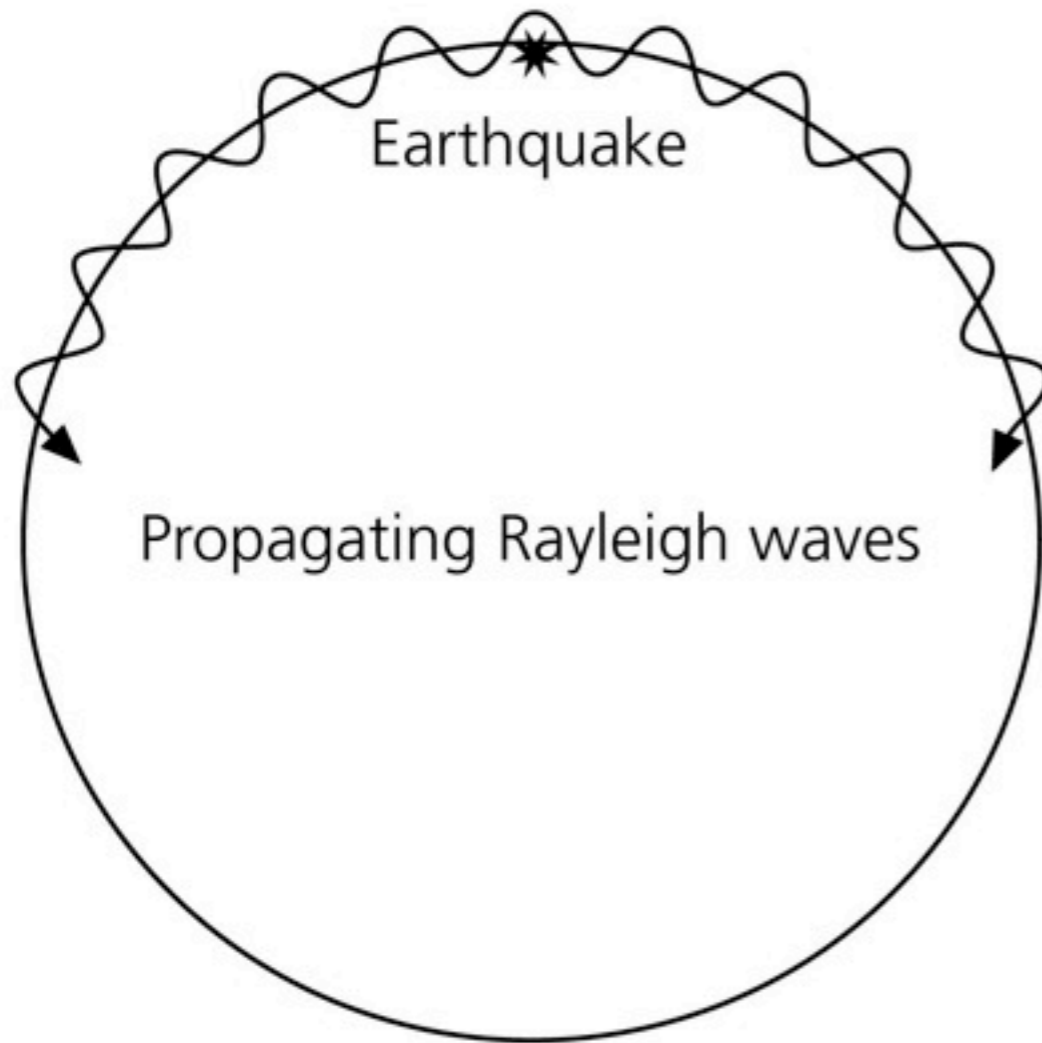
1882 – Lamb – fundamental mode of Earth (as steel ball), 78 minutes

1911 – Love – included self-gravitation – fundamental mode period of 60 minutes

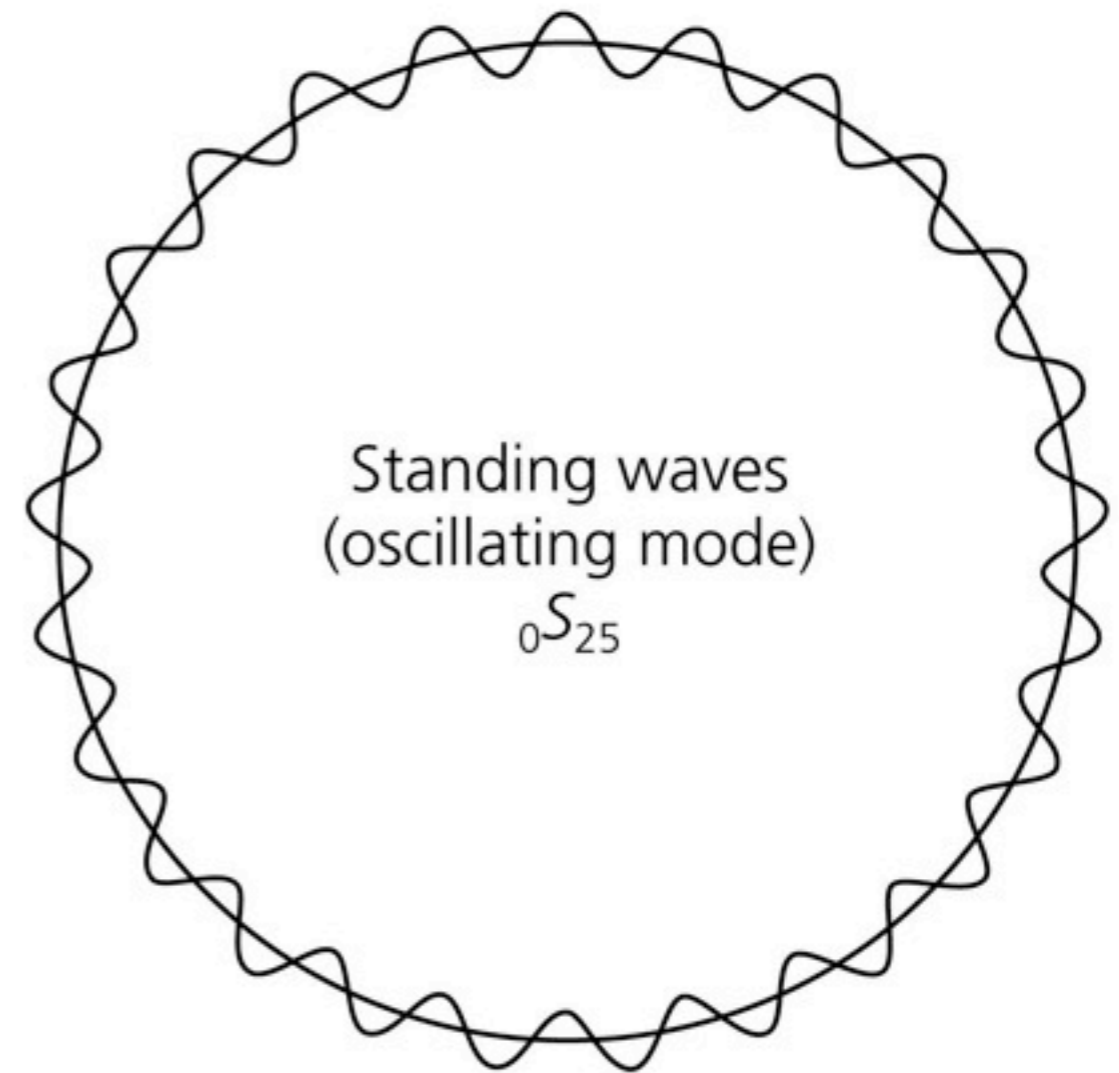
1952 – Kamchatka EQ is first to reveal Earth's normal modes

1960 – Chile earthquake reveals over 40 modes

Figure 2.9-8: Cartoon of the equivalence of surface waves and normal modes.



A few minutes after
the earthquake

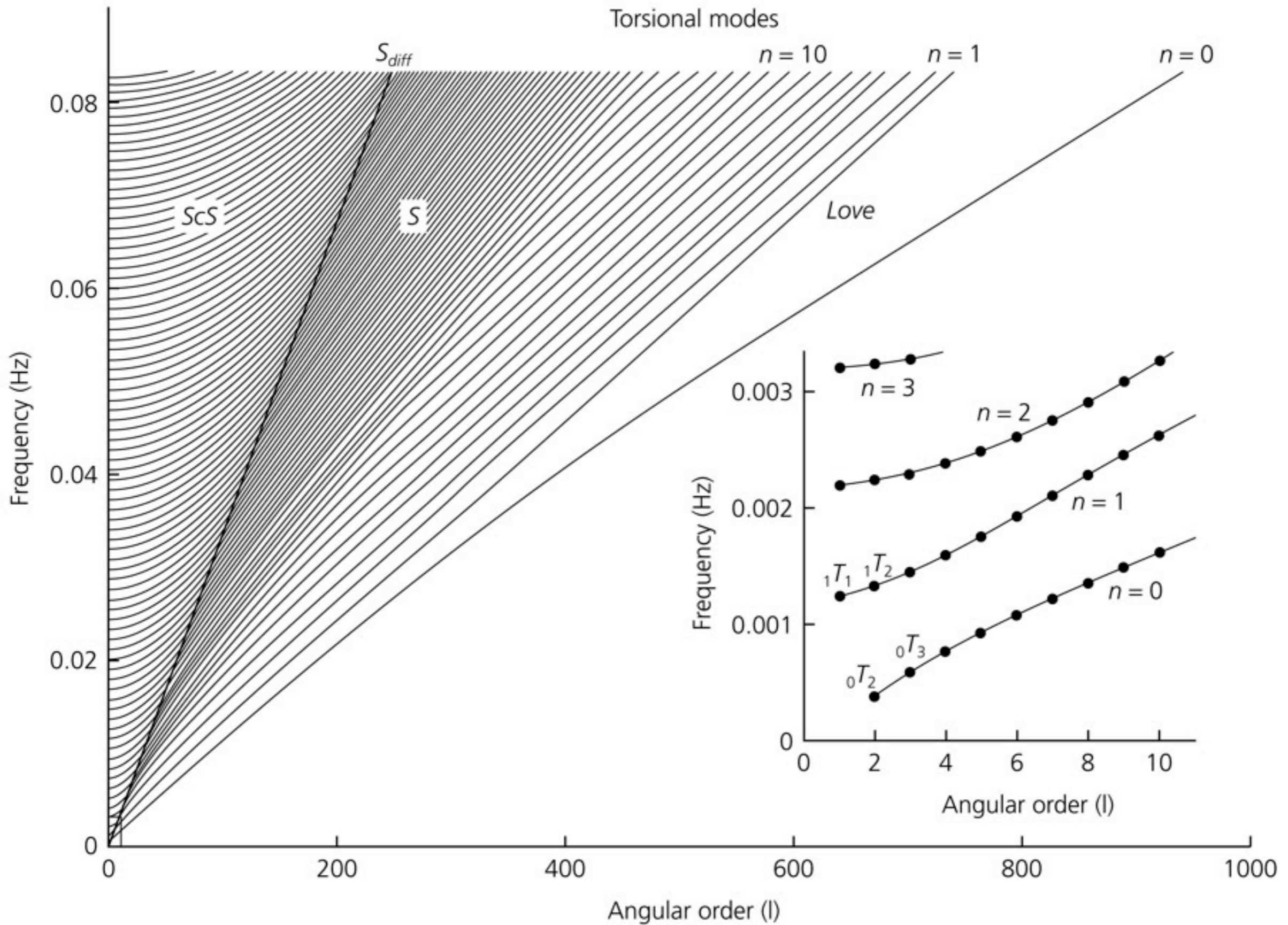


A few hours after
the earthquake

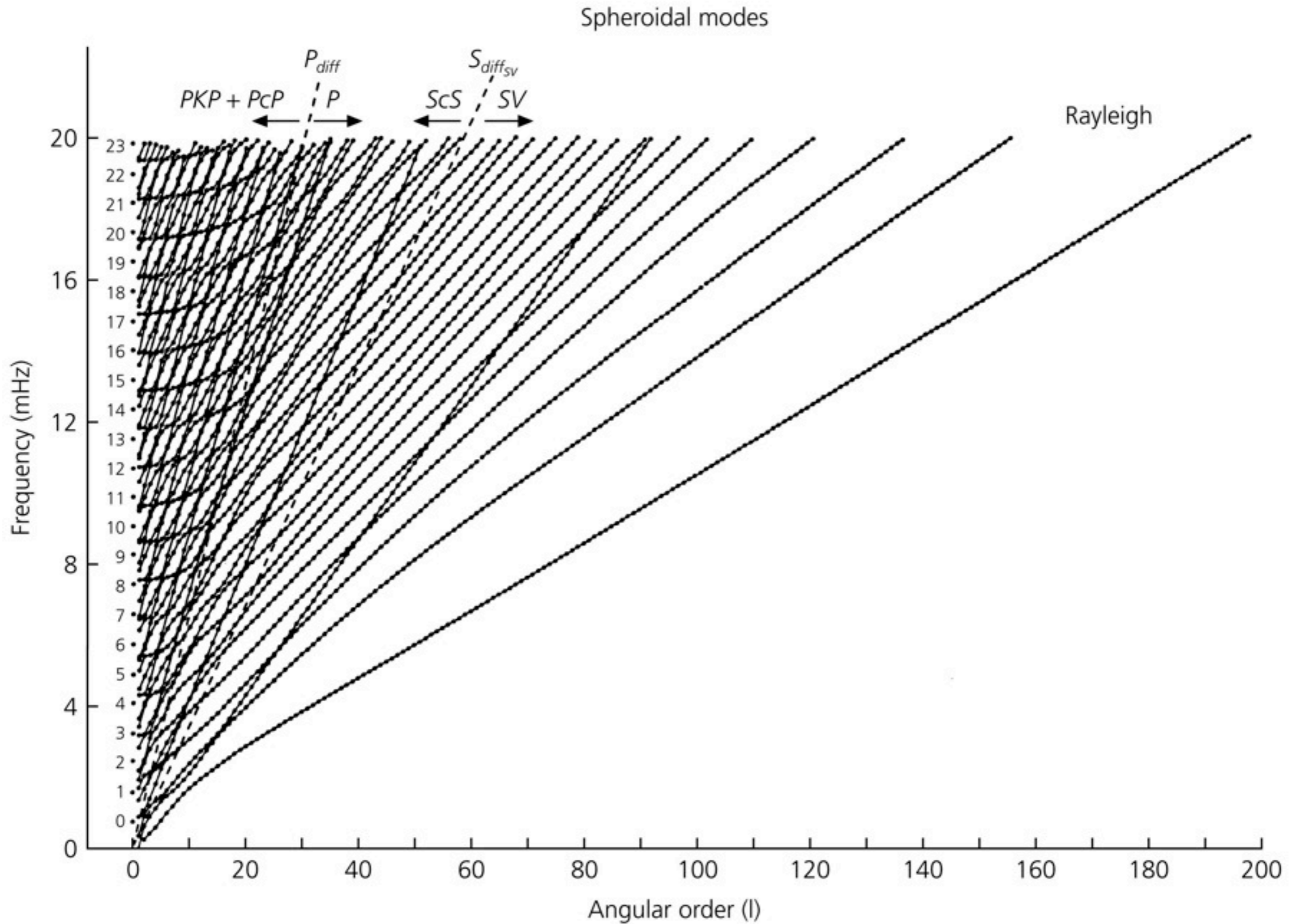
The mode with angular order l and frequency ${}_n\omega_l$ corresponds to a traveling wave with horizontal wavelength $\lambda_x = 2\pi/|\mathbf{k}_x| = 2\pi a/(l + 1/2)$ that has $l + 1/2$ wavelengths around the earth.

These waves travel at a horizontal phase velocity $c_x = {}_n\omega_l/|\mathbf{k}_x| = {}_n\omega_l a/(l + 1/2)$

Torsional modes dispersion

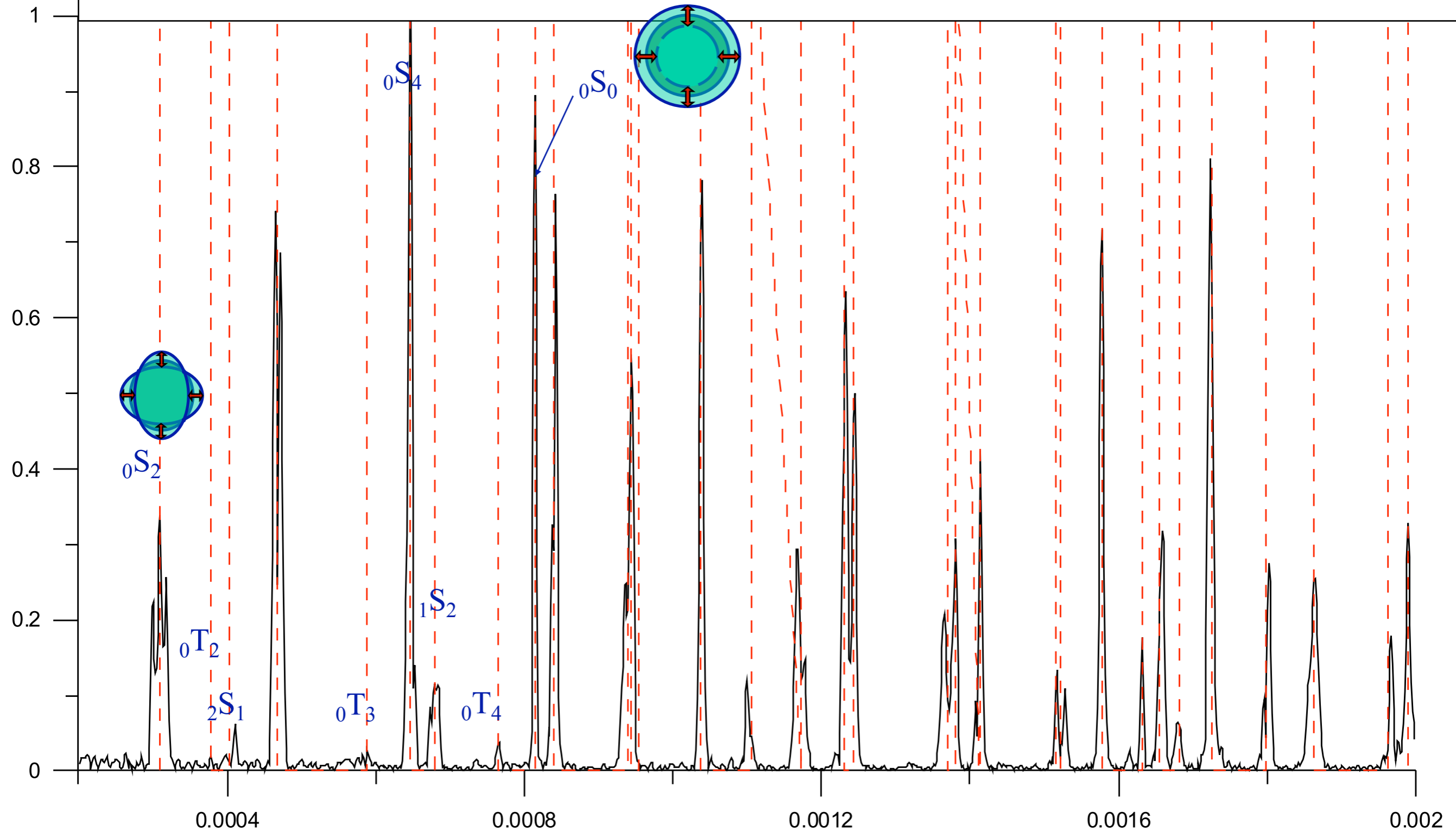


Spheroidal modes dispersion



Sumatra: spectrum

Membach, SG C021, 20041226 08h00-20041231 00h00



Splitting

If SNREI (Solid Not Rotating Earth Isotropic) Earth :

Degeneracy:

for n and l , same frequency for $-l < m < l$

For each m = one singlet.

The $2m+1$ group of singlets = multiplet

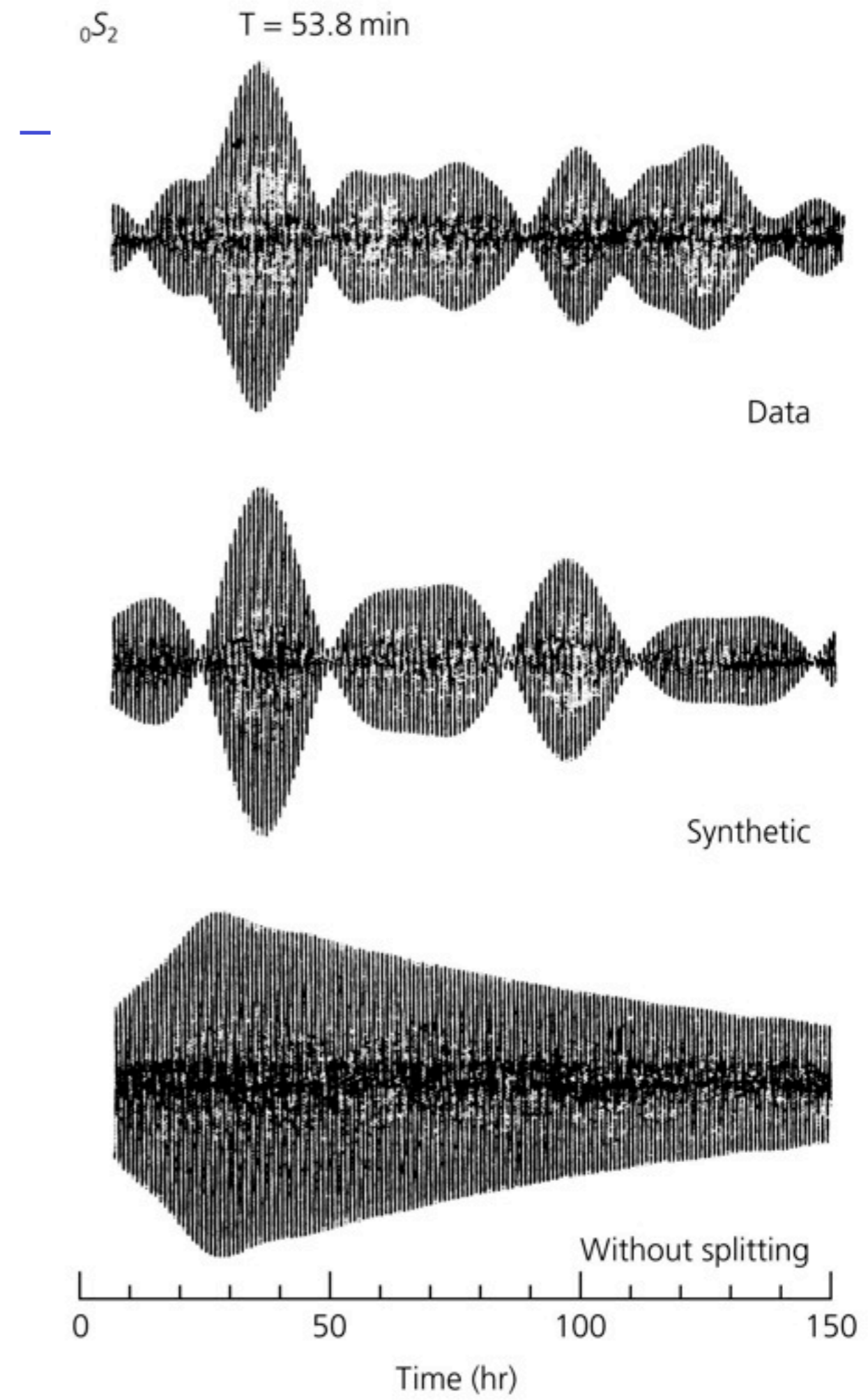
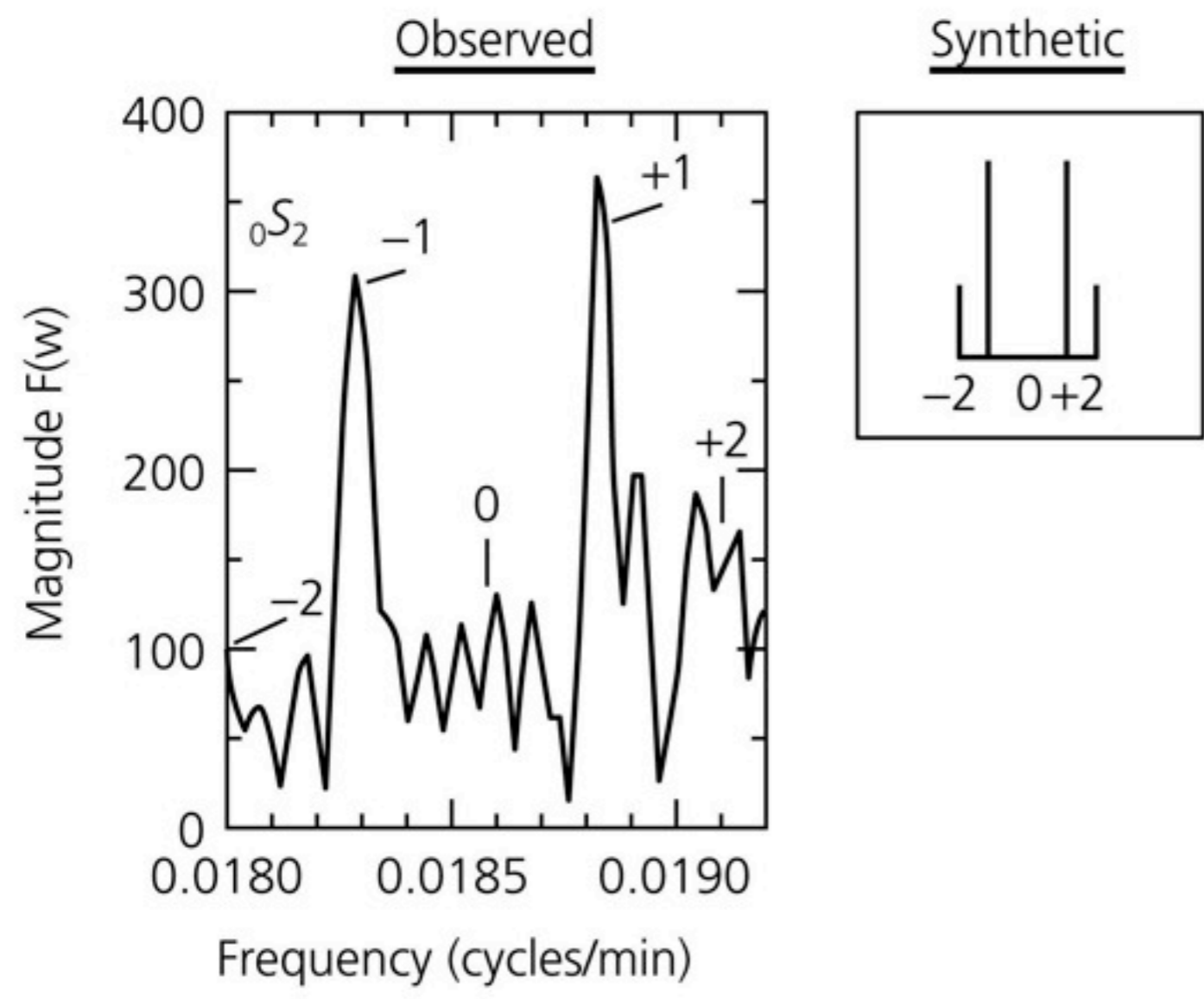
No more degeneracy if no more spherical symmetry :

- * Coriolis
- * Ellipticity
- * 3D

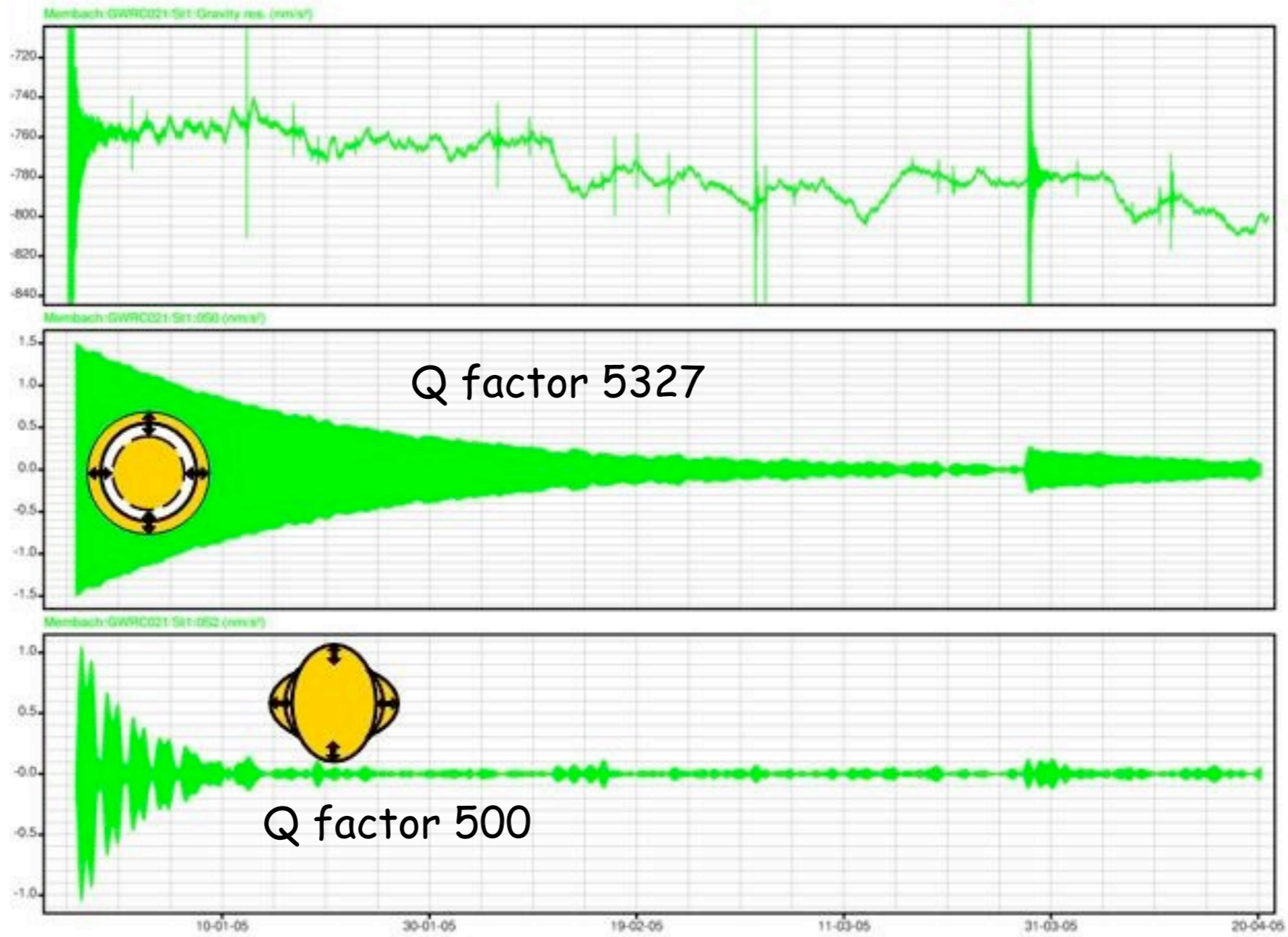
Different frequencies and eigenfunctions for each l, m



Figure 2.9-16: Splitting of the ${}_0S_2$ mode for wave from the 1960 Chile earthquake.



Sumatra: time and Q

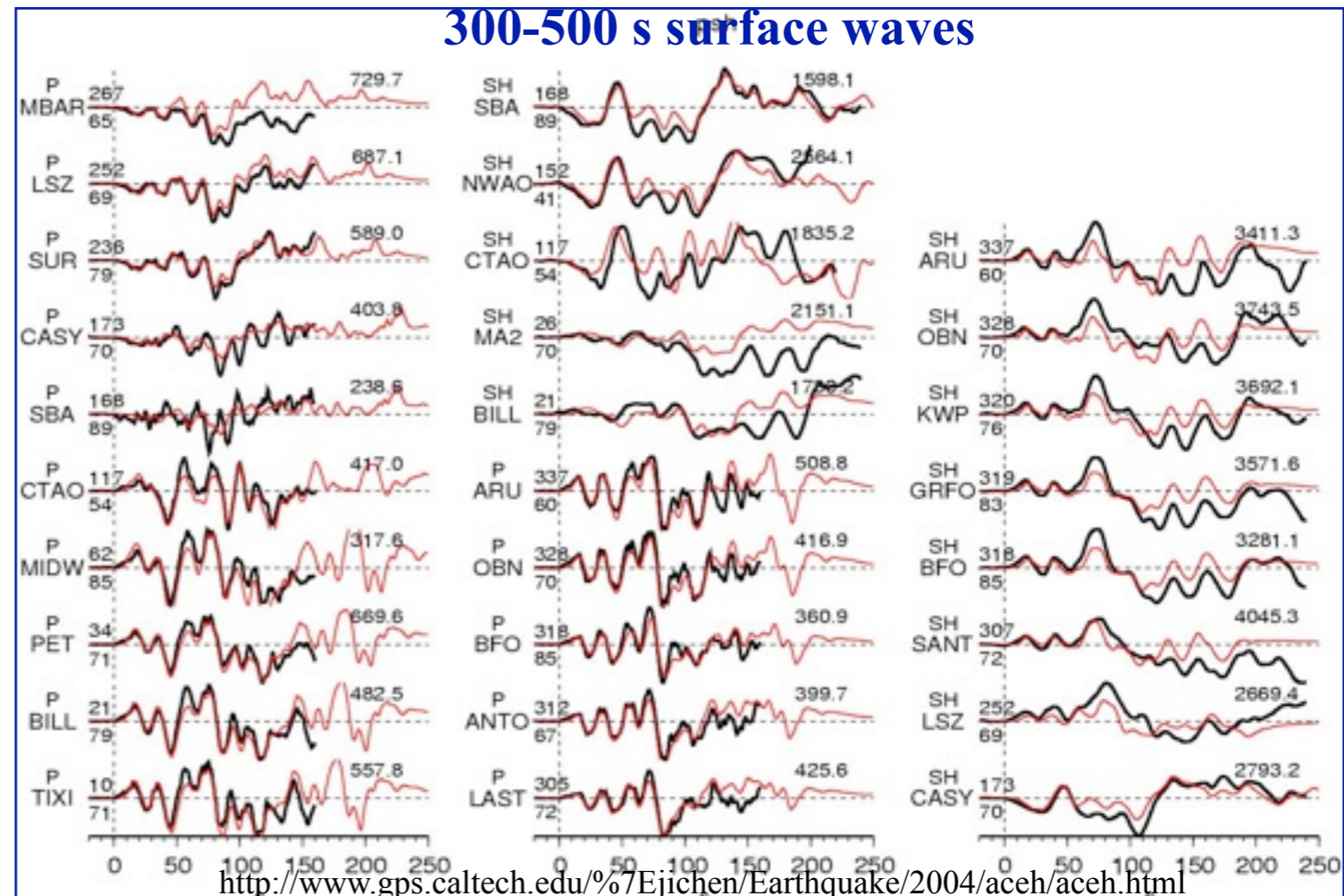


Magnitude

Time after beginning of the rupture:

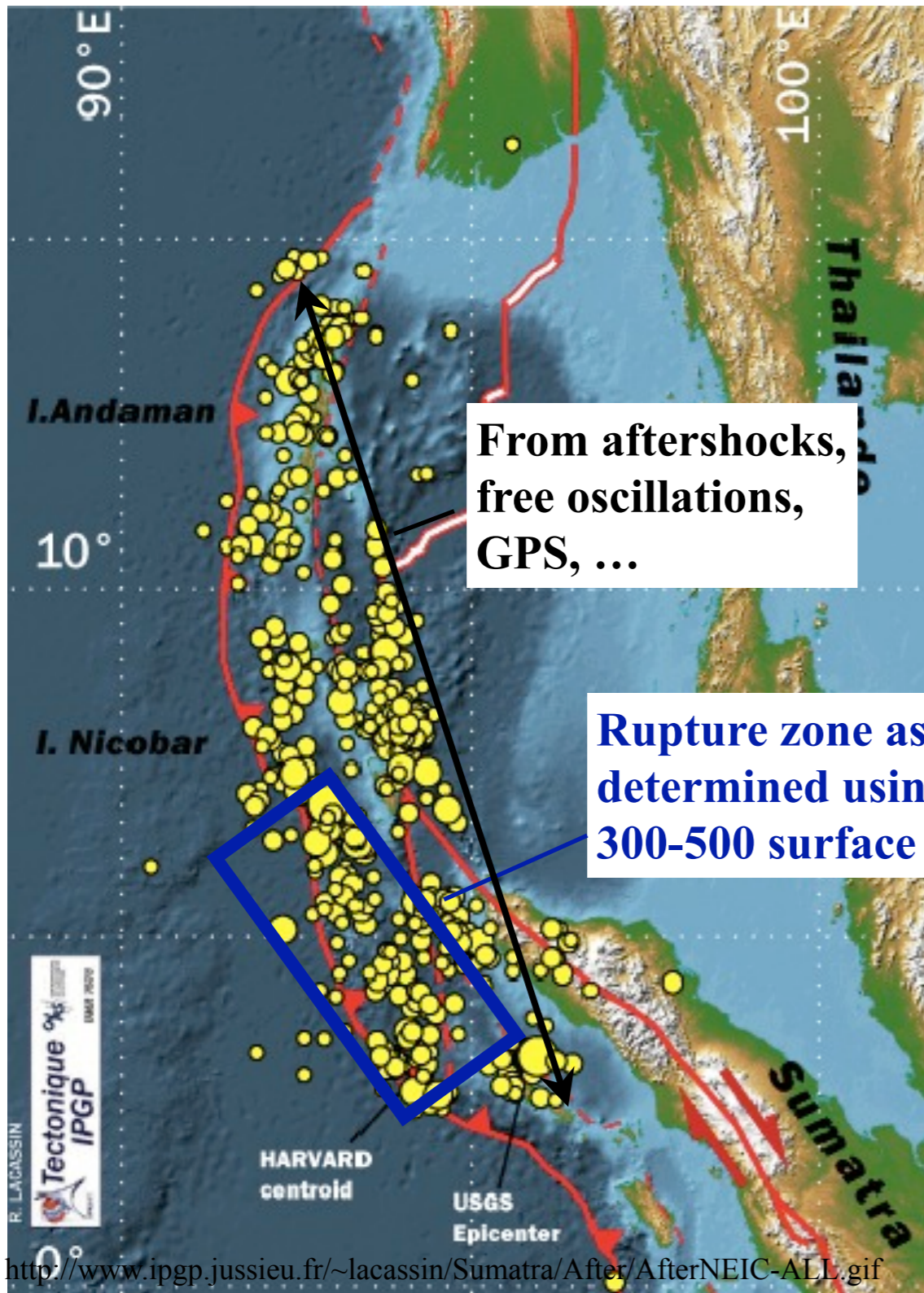
- 00:11 8.0 (M_W) P-waves 7 stations
- 00:45 8.5 (M_W) P-waves 25 stations
- 01:15 8.5 (M_W) Surface waves 157 stations
- 04:20 8.9 (M_W) Surface waves (automatic)
- 19:03 9.0 (M_W) Surface waves (revised)
- Jan. 2005 9.3 (M_W) Free oscillations
- April 2005 9.2 (M_W) GPS displacements

300-500 s surface waves

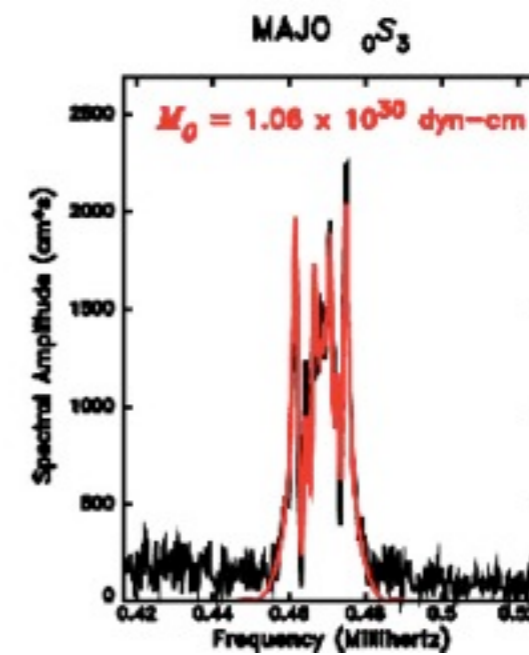
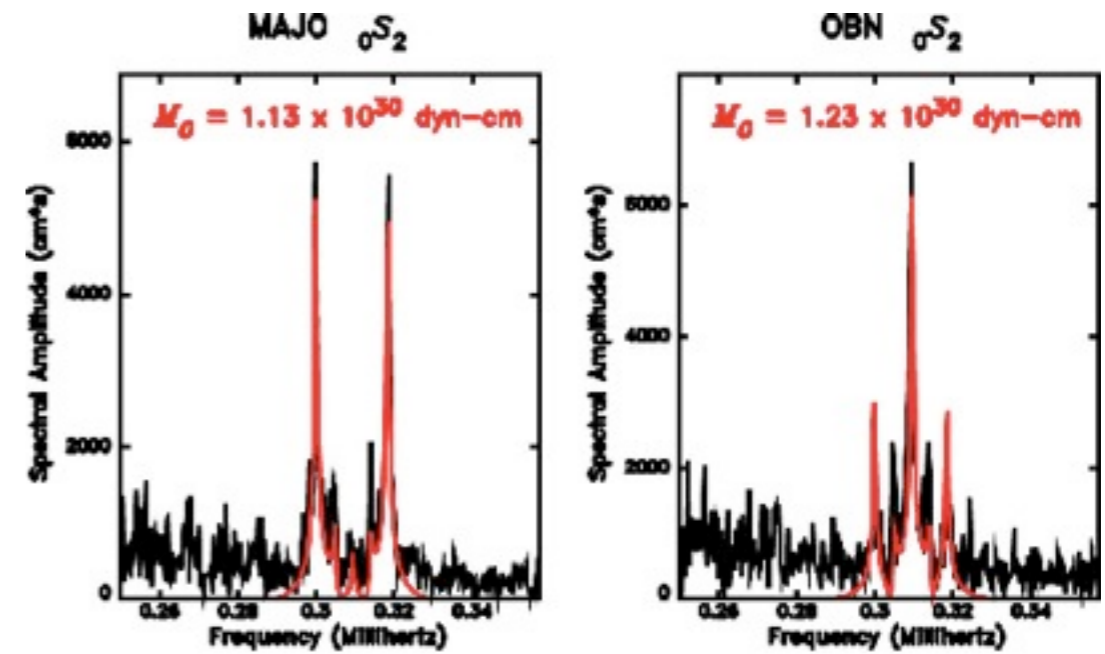


<http://www.gps.caltech.edu/%7Ejichen/Earthquake/2004/aceh/aceh.html>

Magnitude



<http://www.ipgp.jussieu.fr/~lacassin/Sumatra/After/AfterNEIC-ALL.gif>



Seth Stein and Emile Okal
Calculated vs. observed

Modal summation on a sphere

For displacements in 3-D:

$$\mathbf{u}(r, \theta, \phi) = \sum_n \sum_l \sum_m {}_n A_l^m {}_n y_l(r) \mathbf{x}_l^m(\theta, \phi) e^{i \omega_l^m t}$$

n, l, m - radial, angular, and azimuthal orders

${}_n y_l(r)$ - scalar radial eigenfunction

$\mathbf{x}_l^m(\theta, \phi)$ - vector surface eigenfunction

${}_n A_l^m$ - excitation amplitudes (weights for eigenfunctions) that depend on the seismic source.

Modal summation (anelastic)

Normal mode synthetic seismograms:

$$\mathbf{u}^T(r_r, \theta_r, \phi_r) = \sum_n \sum_l \sum_{m=-l}^l {}_n A_l^m(r_s, r_r) {}_n W_l(r_r) \mathbf{T}_l^m(\theta_r, \phi_r) e^{i {}_n \omega_l^m t} e^{-\frac{{}_n \omega_l^m t}{2 {}_n Q_l}}$$

$e^{-\frac{{}_n \omega_l^m t}{2 {}_n Q_l}}$ - the attenuation of the mode

${}_n Q_l$ - quality factor of the mode

After Q cycles of oscillation, the amplitude of a mode has fallen to a level of $e^{-\pi}$ or 4% of the original amplitude.



Figure 2.9-12: Synthesis of a body wave from normal mode summation.

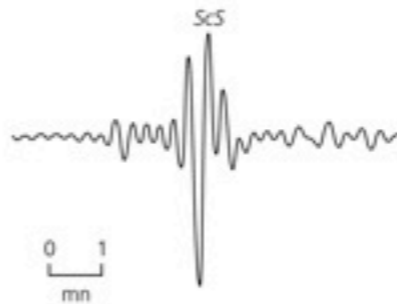
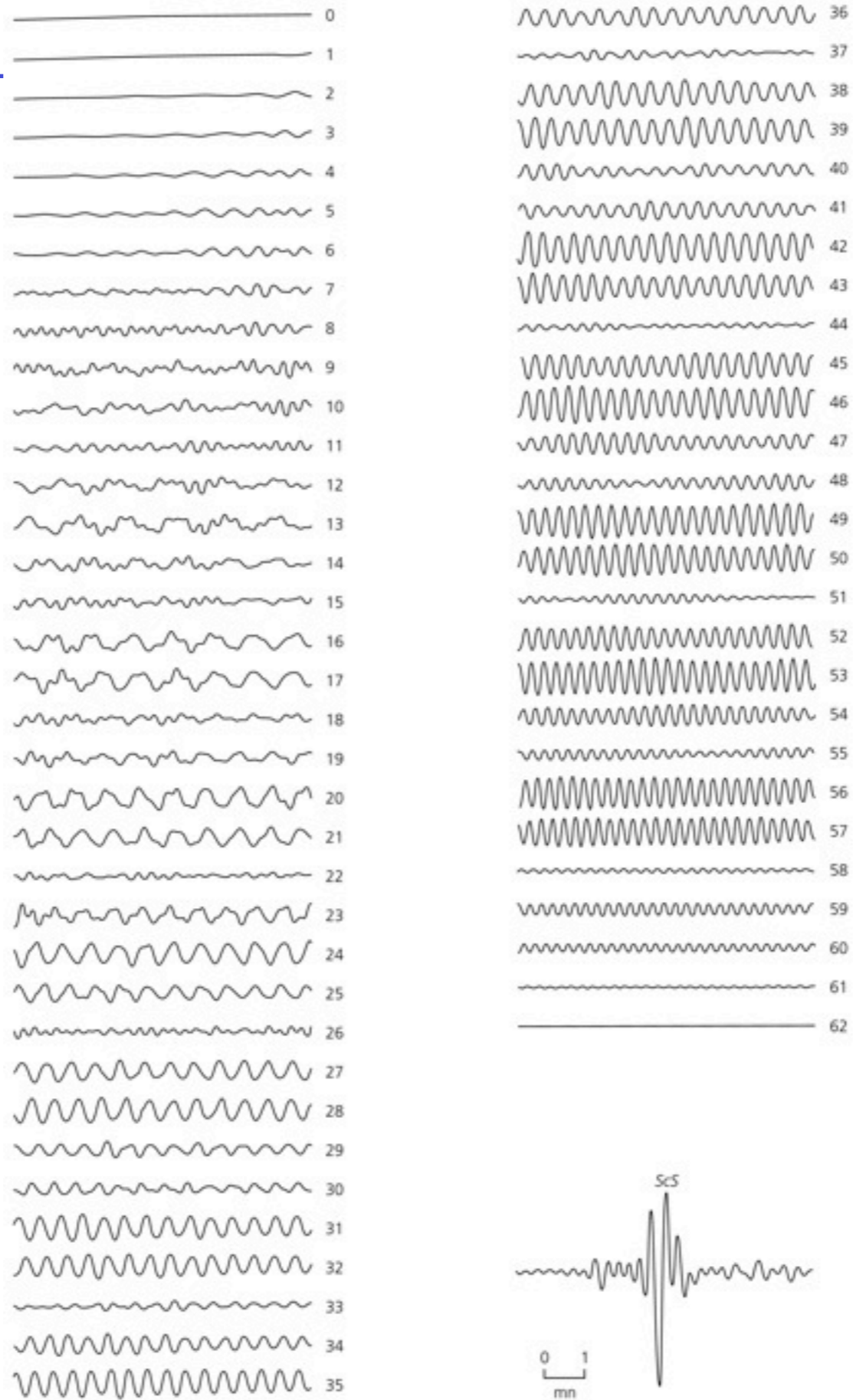
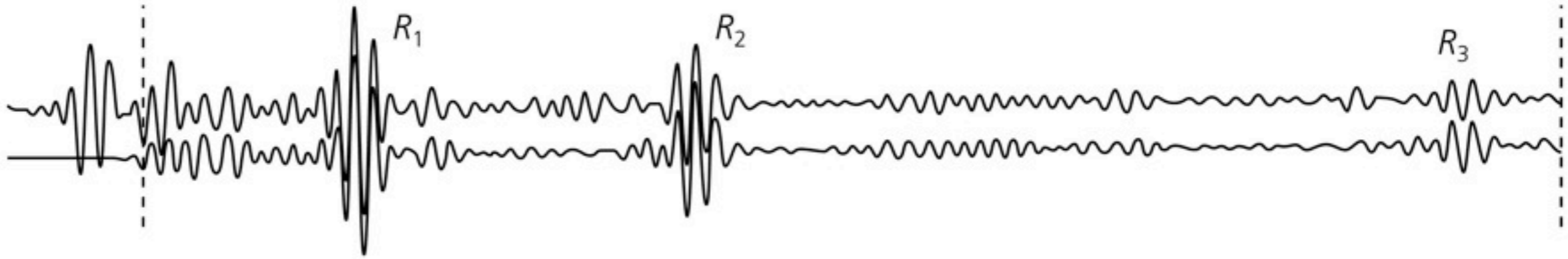


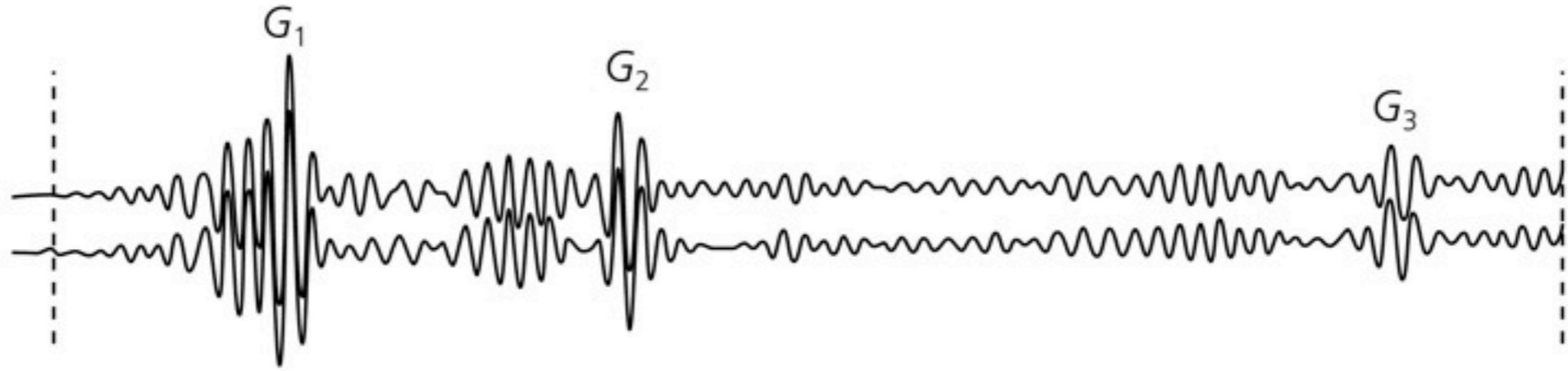


Figure 2.9-13: Example of modeling data with normal mode synthetic seismograms.

STATION ANMO
COMP VERT
DELAY 0.11H
INSTR SRO
DELTA 124.6
AZM AT EP. 52
AMAX 2630



STATION ANMO
COMP N-S
DELAY 0.27H
INSTR SRO
DELTA 124.6
AZM AT EP. 52
AMAX 4352



STATION ANMO
COMP E-W
DELAY 0.20H
INSTR SRO
DELTA 124.6
AZM AT EP. 52
AMAX 2756

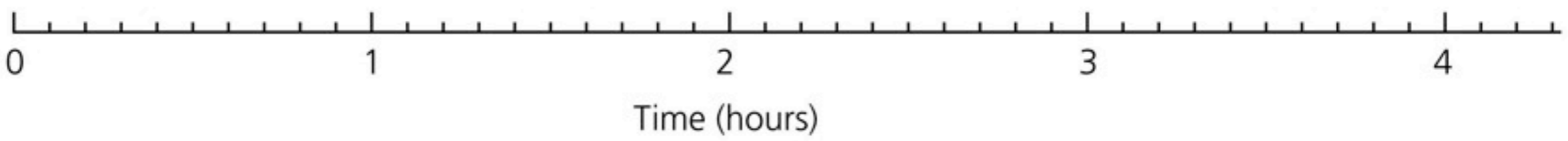
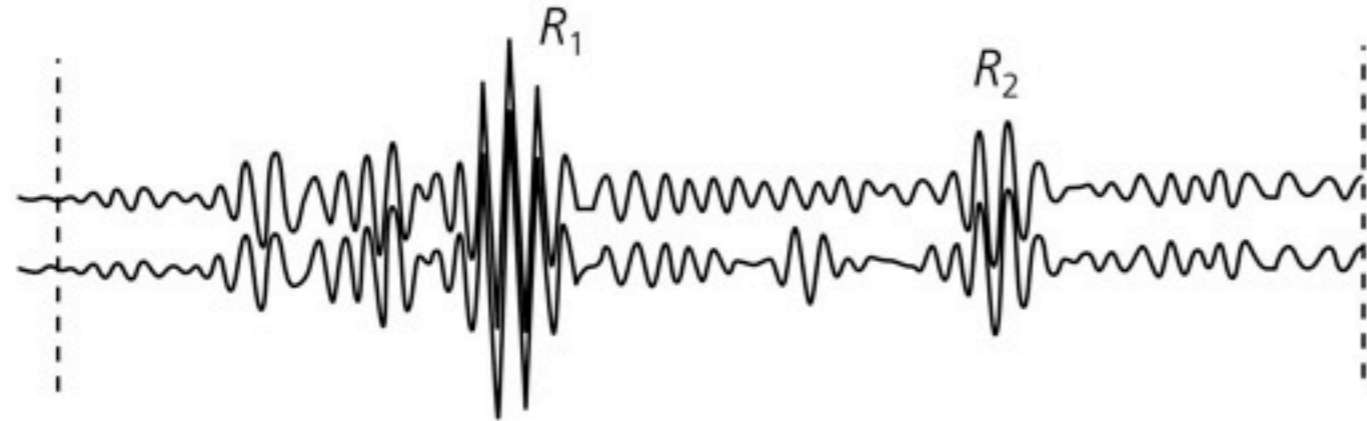


Figure 2.9-14: Shear wave synthetic seismograms computed at a series of depths.

SH displacement at a distance of 70°

